Energy Conversion and Management 166 (2018) 445–462

Contents lists available at ScienceDirect

Energy Conversion and Management

journal homepage: www.elsevier.com/locate/enconman

A multi-objective optimization and multi-criteria evaluation integrated framework for distributed energy system optimal planning

Rui Jing[a], Xingyi Zhu[a], Zhiyi Zhu[b], Wei Wang[a], Chao Meng[a], Nilay Shah[c], Ning Li[a], Yingru Zhao[a,*]

[a] College of Energy, Xiamen University, Xiamen, China
[b] East & West Region, CLP Power Hong Kong Limited, Hong Kong Special Administrative Region
[c] Department of Chemical Engineering, Imperial College London, London, UK

ARTICLE INFO

Keywords:
Distributed energy system
Mixed Integer Non-linear Programming
Solid Oxide Fuel Cell
Multi-objective optimization
Decision making
Multi-criteria evaluation

ABSTRACT

This study proposes an integrated framework for planning distributed energy system with addressing the multi-objective optimization and multi-criteria evaluation issues simultaneously. The framework can be decomposed into two stages. At the optimization stage, the system design and dispatch are optimized considering multiple objectives by Ɛ-constraint method. Three decision making approaches are applied to identify the Pareto optimal solution. At the evaluation stage, a combined Analytic Hierarchy Process and Gray Relation Analysis method is proposed to evaluate and rank various optimal solutions when different objectives and cases are considered. Two stages of work are integrated by introducing the baseline conditions. As an illustrative example, an optimal planning model for a solar-assisted Solid Oxide Fuel Cell distributed energy system is proposed by Mixed Integer Non-linear Programming approach firstly. Then, the system is applied to different cases considering two types of buildings located in three climate zones. The obtained optimal solutions are further evaluated by the proposed multi-criteria evaluation method. Therefore, the overall optimal system design and dispatch strategy, as well as the best demonstration site can be identified comprehensively considering multiple objectives. In general, the results have verified the effectiveness of the proposed framework.

1. Introduction

The problem of fossil fuel depletion is becoming increasingly crucial nowadays due to the growth of world's energy demand. In order to meet the energy demand as well as to limit the production of carbon dioxide, the development of new technologies for energy consumption management and the change from conventional fuel to sustainable fuel are stringent necessity. Recently, attention has been drawn to develop cleaner alternative fuels from renewable resources for the combined cooling, heating and power (CCHP) systems [1]. CCHP is an efficient alternative for building energy supply [2], which draws world-wide attention gradually. Several technologies can be the prime movers of CCHP system including internal combustion engines, gas turbines, Stirling engines, micro turbines and fuel cells [3]. Among all available CCHP prime movers, fuel cells are considered as one of the most promising technologies due to the high energy efficiency and low emissions [4]. Among various types of fuel cells, the Solid Oxide Fuel Cells (SOFCs) are perfect prime movers for the CCHP systems due to intrinsically better electrical efficiency (as high as 60%) and significantly lower pollutant emissions, which makes them a promising alternative for building energy supply [5].

1.1. Literature review

Previous studies have been conducted on modelling the high-level system design and dispatch of CCHP systems to study their feasibility and optimal technique combination. Each study has slightly a different research focus and solves an aspect of the problem from different perspectives.

The MILP (Mixed Integer Linear Programming) and MINLP (Mixed Integer Non-Linear Programming) modelling approaches have been proved by previous studies to be effective ways to solve the design and dispatch optimization problem. Nojavan et al. [6] Proposed an optimal scheduling model for CHP based energy hub considering economic and environmental objectives' trade-offs. Two solving methods, i.e., ε-constraint and max–min fuzzy satisfying, were employed to solve and select the trade-off solution. Zhao et al. [7] proposed a two-stage dispatch optimization model which can tackle the real-time load variation. Jin et al. [8] proposed an MILP model which considers the demand response, meanwhile, day-ahead and adaptive dispatch strategies have been applied to reduce the uncertainty. Ma et al. [9] constructed a MILP model for optimal dispatch of multiple energy systems at micro energy

* Corresponding author.
E-mail address: yrzhao@xmu.edu.cn (Y. Zhao).

https://doi.org/10.1016/j.enconman.2018.04.054
Received 29 November 2017; Received in revised form 10 April 2018; Accepted 14 April 2018

Nomenclature

Abbreviations

ATC	annual total cost
ACE	annual carbon emission
AHP	Analytic Hierarchy Process
ASHP	air source heat pump
BL	baseload
CCHP	combined cooling heating and power
CRF	capital recovery factor
CES	carbon emission saving
GRA	Gray Relation Analysis
HEX	heat exchanger
IEA	International Energy Agency
LINMAP	Linear Programming Technique for Multidimensional Analysis of Preference
LCOE	levelized cost of energy
MINLP	Mixed Integer Non-linear Programming
MILP	Mixed Integer Linear Programming
OPEX	operating expenditures
OPEXS	operating expenditure saving
OEF	on-site energy fraction
OEM	on-site energy matchness
OEP	on-site energy performance
SOFC	solid oxide fuel cell
SRI	solar radiation index
TOPSIS	Technique for Order Preference by Similarity to an Ideal Solution

Symbols

AM	air mass
A	area (m^2)
C	cost ($)
CAP	installed capacity (kW)
d	deviation index
E	electrical power (kW)
ED_{i+}	distance to ideal point
ED_{i-}	distance to non-ideal point
f	part load efficiency function
f_{ij}^{norm}	location of each optimal point
f_j^{ideal}	location of ideal point
$f_j^{\text{n- ideal}}$	location of non-ideal point
h	hour
PL	part load ratio
Y_i	relative distance
Q	thermal energy (kW)
T	temperature (°C)

Greek symbols

ω	heat-to-power ratio
η	efficiency
α	charge/discharge status
δ	import/export status
β	on/off status
φ	start limit variable
∂	emission factor
μ	energy conversion factor

Subscripts/superscript

ac	absorption chiller
b	boiler
cap	capital cost
cool	cooling energy
chr	heat storage charge
dis	heat storage discharge
ec	electrical chiller
ex	electricity export
fc	solid oxide fuel cell
h	hour
heat	heating energy
hp	heat pump
im	electricity import
LHV	low heating value
limit	installed capacity limit
maint	maintenance cost
NG	natural gas
n	project life
pv	photovoltaic
re	heat recovered
r	interest rate
s	season
st-in	energy flow into storage
st-out	energy flow out storage
t	each technology
tc	thermal collector

grid level. Electricty, heating and cooling were coordinated by day-ahead dynamic operational optimization. Demand response were enabled as well. Kang [10] proposed a ground source heat pump assisted CCHP system and discussed the impacts of electricity feed-in tariff and carbon tax on system design and dispatch. Facci [11] designed a SOFC based CCHP system and applied in a residential building. The system design capacities have been fitted as a function of capital cost based on different control strategies.

These studies aim to optimize the system for either economic or environmental objectives. Meanwhile other studies analyzed the trade-off between more than one objective by multi-objective optimization approaches. Saman et al. [12] modelled a solar and wind assisted SOFC CCHP system considering cost, emissions and area as objectives simultaneously. Zhang et al. [13] established a MILP model for optimal dispatch of the UK domestic energy supply system as well as optimal scheduling of the home appliances to achieve least operation cost or carbon emissions. Ju [14] optimized a CCHP system by considering four objectives and entropy weighting was applied to assign weights for each objective. Wei [15] utilized NSGA-II (Non-dominated Sorting Genetic Algorithm-II) to optimize the system operation parameters for the objectives of maximizing energy saving and minimizing energy cost.

Except for optimization of the design and dispatch research, other researchers use multi-criteria assessment approaches to evaluate the feasibility of distributed energy system particularly for comparison purposes. Li et al. [2] applied the entropy weighting approach to assign weights when comparing different criteria from different cases. Wu et al. [16] compared the CHP system performance when implemented in Japan and China by an improved GRA approach. Wang et al. [17] utilized a combined AHP and entropy weighting approach to assess the performance of different prime movers for CCHP systems.

It can be seen that some of the researches focused on optimization of distributed energy system by considering dispatch optimization only, while the optimal design issue may not be tackled. Some researchers conducted the multi-objective optimization by only one approach or not mentioned the decision making details. Other researches focused on performance comparison, but the optimization models may relatively

be simplified.

1.2. Motivation

Based on the literature review, this study proposes a framework, which aims to (1) tackle the design and dispatch optimization issue, (2) conduct multi-objective optimization by different approaches, (3) combine the optimization model with an evaluation model. Before the description of the proposed optimization and evaluation framework, one issue should be clarified in the first place - what is the relation between "multi-objective optimization" and "multi-criteria evaluation" research? The similarities are (1) they both consider certain "targets", which are called "objectives" in optimization and "criteria" in evaluation, these "targets" always have trade-offs between each other and cannot achieve best values simultaneously, (2) they both involve "performance comparison", which means the comparison among each case or scenario. However, the difference between them is implicit. In the distributed energy system planning aspect, the "multi-objective optimization" aims to optimize the "objectives" through establishing an optimization model, where the input parameters to the optimization model are the same for each run. Thus different optimized results are defined as "scenarios" in this study, which depend on different objectives. By contrast, the "multi-criteria evaluation" aims to identify the best "case" among all "cases", the input parameters are different for each case, thus the system performance relies on the variation of inputs, and the introduced criteria are dimensionless in general for comparison purposes. In this study, a framework of combined "multi-objective optimization" and "multi-criteria evaluation" has been proposed and an explanatory schematic has been presented in Fig. 1. The framework can be divided into two stages. (1) At the optimization stage, where a MINLP optimization model has been built in the first place. Then annual total cost (ATC) and annual carbon emissions (ACE) are considered as objectives and the optimization result for each objective is defined as a "scenario". It is straightforward to compare "obj 1" solution to "obj *n*" solution in same "case". However, the comparison between the "obj 1" solution in one scenario and another "obj 1" solution in other "cases" cannot be conducted directly. (2) Therefore, at the evaluation stage, the problem of comparison between different "cases" is tackled by introducing baseline conditions. Then, different dimensionless criteria can be defined so as to compare the solutions between different "cases" and further identify the best case. Taking the case study conducted in this paper, the proposed system is applied to totally six "cases" including hotels and hospitals located in Beijing, Shanghai and Xiamen respectively. Within one "case" such as "a hotel in Beijing", the input parameters to the optimization model such as climate conditions, energy demand and energy prices are same for each "scenario", thus the optimal result's difference depends on either optimizing the system for the least cost or carbon emissions or both. However, the optimization results for a hotel in Beijing cannot be directly compared to those of a hospital in Shanghai obviously as two completely different "cases". In order to identify which building type and location is the best demonstration site for the proposed system, several dimensionless criteria have been introduced by considering conventional energy system performance as baselines, thus the criteria can be defined such as cost saving rate or carbon emission saving ratio. Then the performance between each case can be further compared through the proposed evaluation model.

In general, previous research is focused on either different "cases" or "scenarios", which are not contradictory. In this study, a novel integrated framework for optimization and evaluation is proposed, which considers "scenarios" and "cases" simultaneously as two stages. In the optimization stage, the optimal scenarios are determined with different objectives. Then in the evaluation stage, through introducing the baseline conditions as the linkage, both the best case and the best scenario can be identified by several dimensionless criteria. Therefore, the overall best case and scenario can be determined, meaning that the optimal system design and dispatch strategy as well as the best implementation site of the proposed system can be determined.

Compared to previous work, the major contributions have been listed as follows:

- Clarify the relationship between multi-objective optimization and multi-criteria evaluation.
- Present a novel framework combining multi-objective optimization and multi-criteria evaluation approaches to tackle the optimal planning issue of distributed energy system.
- Establish a MINLP model for optimal design and dispatch of a hybrid solar assisted SOFC-CCHP system with particularly designed constraints (e.g., part-load ratio, ramp up/down and maximum start limit) to make the model more practical.
- Conduct multi-objective optimization by $\mathcal{E}$-constraint method, implement three well-known approaches for decision making, and further compare the effectiveness of each decision making approaches and identify their applicability.
- Propose a novel multi-criteria evaluation approach via the integration of AHP and GRA approaches.

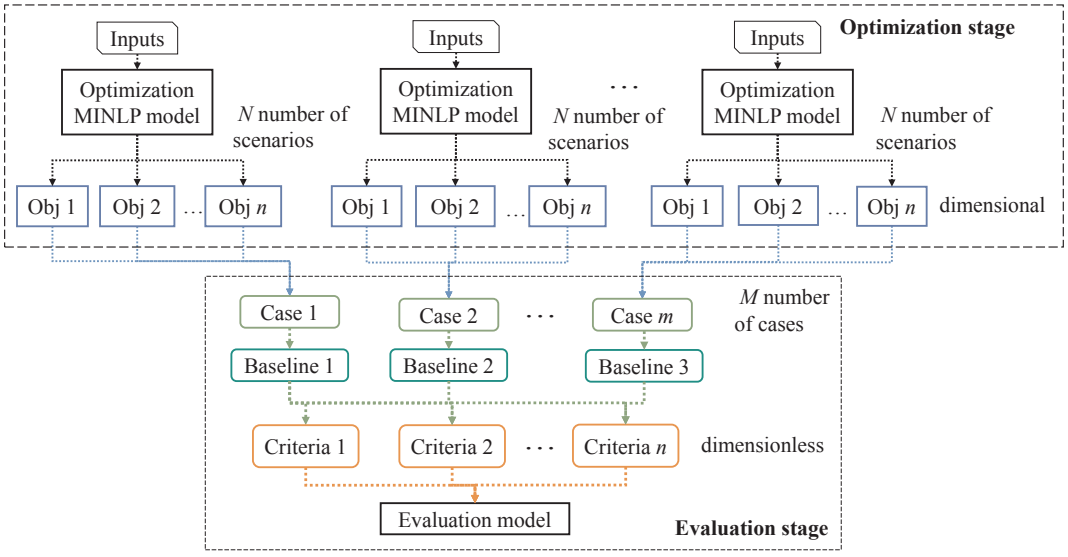

Fig. 1. Illustrative overview of the problem.

The paper has been organized as follows: Section 2 clarifies the problem as well as the proposed technical roadmap, Section 3 describes the established MINLP model and constraints in detail, Section 4 introduces multi-objective optimization and three decision making approaches, Section 5 proposes the novel evaluation approach, Section 6 implements the proposed models and approaches to case studies, Section 7 discusses the results, and Section 8 draws some conclusions.

2. Problem and solutions description

As mentioned in the motivation section, this study proposes an optimization and evaluation framework to tackle the hybrid SOFC-CCHP system mid-term (10 years) planning problem, in which the framework can be further divided into four parts: (1) pre-process inputs, (2) optimization, (3) multi-objective and decision making, (4) evaluation. For each part, certain solutions have been implemented, an overview of technical roadmap for this study has been presented in Fig. 2.

(1) Pre-process inputs

Before the optimization stage, the input parameters should be prepared from technical, economic, environmental and climate perspectives. The accuracy of inputs has a direct impact on the system design and operating performance [8]. Therefore, the economic and technical parameters are based on well-documented technologies as well as corresponding research. The weather data such as temperature, solar radiation index have been downloaded from the National Meteorological Administration [18]. In this study, since the focus is the optimization and evaluation model, it is assumed that the loads are given based on previous research as well as reasonable assumptions.

(2) Optimization

At the optimization stage, the aim is to determine the best technique combination of the hybrid SOFC-CCHP system by optimizing the installed capacity of each device. Meanwhile, the optimal dispatch strategy is also determined based on the objectives. Note that it is important to solve the design and operational models together in dynamic systems. To achieve these goals, a MINLP model has been established and described in detail at the following section.

(3) Multi-objective and decision making

In this study, the approach to conduct multi-objective optimization has been introduced to analyze the trade-off between different objectives. Three well-known decision making approaches (LINMAP, TOPSIS, Shannon Entropy) have been applied to identify the final desired solution and the effectiveness of these approaches has been discussed.

(4) Evaluation

After applying the proposed optimization model to different cases, the performance comparison requires a comprehensive evaluation tool, which considers different criteria with varying scales simultaneously. In this study, a combined AHP and GRA evaluation approach has been proposed, which not only considers the subjective preference of the decision maker, but also the objective differences among each cases.

3. Optimization model description

In this section, a solar assisted solid oxide fuel cell (SOFC) distributed energy system is proposed to serve the building's electrical, heating, and cooling demand. The optimization objectives as well as model constraints are presented in detail.

3.1. System overview

The proposed system is assumed to have its own heating and cooling network, and a local micro electrical network which is also available to interact with the grid. The potential devices include: solid oxide fuel

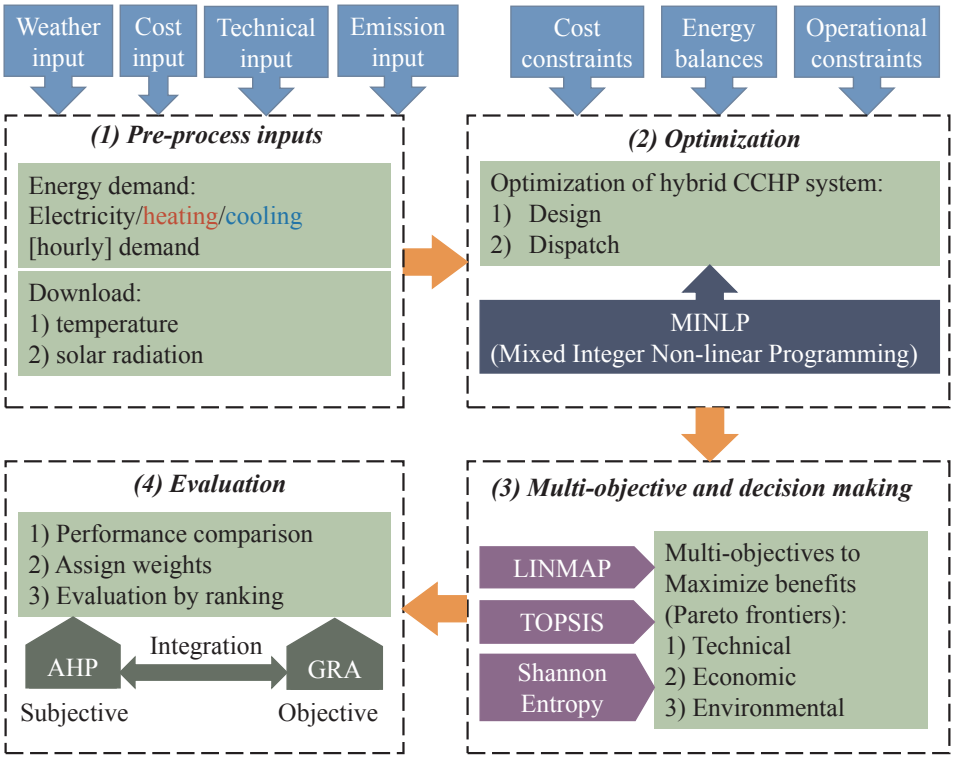

Fig. 2. Technical roadmap of the proposed optimization and evaluation framework.

cell (SOFC) unit, boiler, heat recovery unit, heat storage tank, absorption chiller, air source heat pump (ASHP), electrical chiller, solar photovoltaic panel (with battery), and solar thermal collector as presented in Fig. 3, where pre-heated natural gas, compressed air and water are fed into the SOFC with stack temperature of around 1073 K [19]. Reforming reactions are considered inside the SOFC stack [20]. Then the exhaust gas containing un-reacted fuel is further burnt by an afterburner. Upstream of the fuel cell, the fuel, air and water is pre-heated by heat exchangers to around 800 K. Then the residual heat of the exhaust gas (at around 750 K) is further recovered for heating by a heat exchanger, or for cooling by connecting to an absorption chiller. Meanwhile, renewable solar energy has been fully utilized by both PV panel and solar thermal collector. Besides, an air source heat pump is also available if necessary to further improve the system's efficiency as well as the environmental performance.

In order to tackle the optimal design and dispatch problem, a MINLP model has been built. To make the model perform closer to the practice, several unique constraints have been imposed and explained as follows.

3.2. Energy balances

The energy balances consist of electrical balance, heating balance and cooling balance. In the electrical balance, the electrical demand is fulfilled by electricity supplied from solar PV panel, generated from SOFC, imported from grid and battery discharge, minus possible consumption by electrical chiller and heat pump, battery charge or export to grid as shown in Eq. (1).

$$E_{\text{demand},s,h} = E_{\text{pv},s,h} - E^{\text{bat}}_{\text{st-in},s,h} + E^{\text{bat}}_{\text{st-out},s,h} + E_{\text{fc},s,h} + E_{im,s,h} - E_{\text{ex},s,h} - E_{\text{ec},s,h} - E_{\text{hp},s,h} \quad \forall\, s,h \tag{1}$$

The heat demand is fulfilled by the solar thermal collector, recovered heat from SOFC, gas boiler, air source heat pump, interaction with heating storage and minus possible heat consumption by absorption chiller as presented in Eq. (2).

$$Q^{\text{heat}}_{\text{demand},s,h} = Q^{\text{heat}}_{\text{tc},s,h} + Q^{\text{heat}}_{\text{r},s,h} + Q^{\text{heat}}_{\text{b},s,h} - Q^{\text{heat}}_{\text{st-in},s,h} + Q^{\text{heat}}_{\text{st-out},s,h} + Q^{\text{heat}}_{\text{hp},s,h} - Q^{\text{heat}}_{\text{ac},s,h} \quad \forall\, s,h \tag{2}$$

The cooling demand is supplied by either electrical chiller, absorption chiller or both as illustrated in Eq. (3).

$$Q^{\text{cool}}_{\text{demand},s,h} \leqslant Q^{\text{cool}}_{\text{ac},s,h} + Q^{\text{cool}}_{\text{ec},s,h} \quad \forall\, s,h \tag{3}$$

The power exchange between the grid and the hybrid SOFC-CCHP system is defined by Eq. (4) and electricity feed-in is prohibited during the night off-peak period.

$$0 \leqslant E_{\text{ex},s,h} \leqslant \delta_{\text{ex},s,h} \times E^{\text{limit}}_{\text{ex}} \quad \forall\, s,h \tag{4a}$$

$$0 \leqslant E_{\text{im},s,h} \leqslant \delta_{im,s,h} \times E^{\text{limit}}_{\text{im}} \quad \forall\, s,h \tag{4b}$$

$$\delta_{\text{ex},s,h} + \delta_{im,s,h} \leqslant 1 \tag{4c}$$

$$E_{\text{ex},s,h} = 0 \quad \forall\, s \text{ and } h \in (0,7) \tag{4d}$$

where $\delta_{\text{ex},s,h}$ and $\delta_{im,s,h}$ are binary variables to control the power exchange and to avoid power export and import simultaneously.

3.3. Capacity constraints

Each installed device has a capacity limit (CAP^{limit}) which prevents over size of installed capacity, and also benefits the model solving time as shown in Eq. (5). Meanwhile, the thermal output and energy balances of electrical chiller, absorption chiller, heat pump, and boiler are calculated by Eqs. (6) and (7), where β is a binary variable to control the on/off status of certain devices, η represents each device' efficiency, CAP denotes the installed capacity, and PL is the part load ratio of each device at each time step accordingly. Since both CAP and PL are variables, the problem requires a non-linear model with integer variables.

$$CAP_t \leqslant CAP^{\text{limit}}_t \quad \forall\, s,h \tag{5}$$

$$Q^{\text{cool}}_{\text{ec},s,h} = \beta_{\text{ec},s,h} \times CAP_{\text{ec}} \times PL_{\text{ec},s,h} \quad \forall\, s,h \tag{6a}$$

$$Q^{\text{cool}}_{\text{ac},s,h} = \beta_{\text{ac},s,h} \times CAP_{\text{ac}} \times PL_{\text{ac},s,h} \quad \forall\, s,h \tag{6b}$$

$$Q^{\text{heat}}_{\text{hp},s,h} = \beta_{hp,s,h} \times CAP_{\text{hp}} \times PL_{hp,s,h} \quad \forall\, s,h \tag{6c}$$

$$Q^{\text{heat}}_{b,s,h} = \beta_{b,s,h} \times CAP_{\text{b}} \times PL_{b,s,h} \quad \forall\, s,h \tag{6d}$$

$$Q^{\text{cool}}_{\text{ec},s,h} = \beta_{\text{ec},s,h} \times \eta_{\text{ec}} \times E_{\text{ec},s,h} \quad \forall\, s,h \tag{7a}$$

$$Q^{\text{cool}}_{\text{ac},s,h} = \beta_{\text{ac},s,h} \times \eta_{\text{ec}} \times Q^{\text{heat}}_{\text{ac},s,h} \quad \forall\, s,h \tag{7b}$$

$$Q^{\text{heat}}_{\text{hp},s,h} = \beta_{hp,s,h} \times \eta_{\text{hp}} \times E_{\text{hp},s,h} \quad \forall\, s,h \tag{7c}$$

$$Q^{\text{heat}}_{b,s,h} = \beta_{b,s,h} \times \eta_{\text{b}} \times NG_{b,s,h} \quad \forall\, s,h \tag{7d}$$

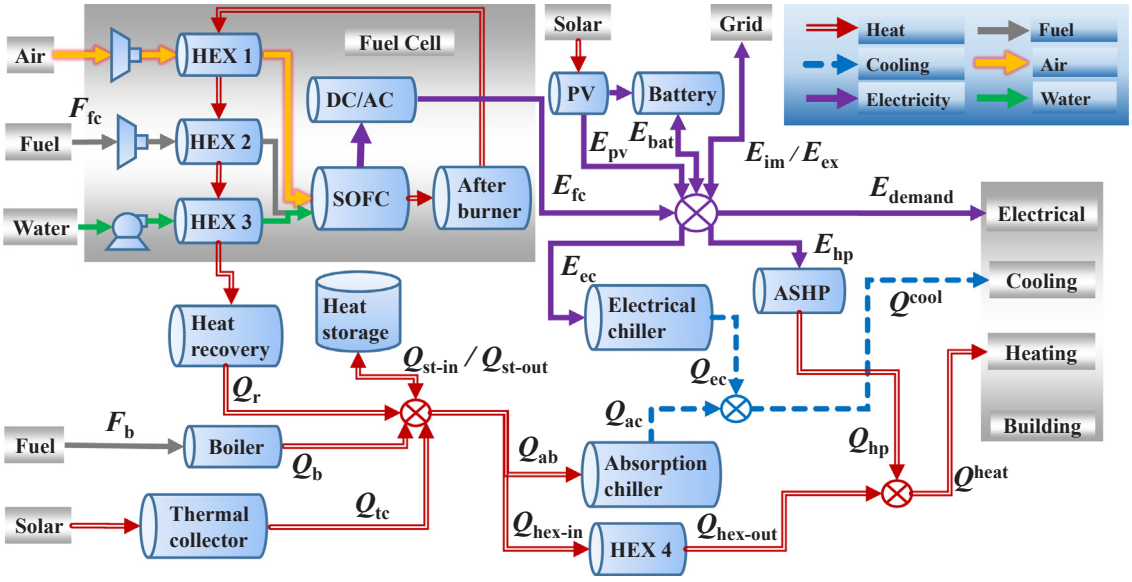

Fig. 3. Schematic of a hybrid SOFC-CCHP system.

3.4. Energy storage constraints

Both electrical and thermal storage are considered in this study.

3.4.1. Thermal storage

The heat stored in a tank at time $h+1$ is equal to the amount of stored heat at h plus the heat charged minus the heat discharged [21]. The heat energy losses during the charge/discharge process as well as in the tank have been considered, and the heat charge and discharge cannot happen simultaneously by introducing binary variable α to control the status of charge/discharge.

$$Q^{\text{heat}}_{\text{st},s,h} \leqslant CAP^{\text{limit}}_{\text{st}} \quad \forall\, s,h \tag{8a}$$

$$Q^{\text{heat}}_{\text{st},s,h+1} = \eta^{\text{heat}}_{\text{st}} \times Q^{\text{heat}}_{\text{st},s,h} + \eta^{\text{heat}}_{\text{st-in}} \times Q^{\text{heat}}_{\text{st-in},s,h+1} - Q^{\text{heat}}_{\text{st-out},s,h+1} / \eta^{\text{heat}}_{\text{st-out}} \quad \forall\, s \text{ and } h \in (1,23) \tag{8b}$$

$$Q^{\text{heat}}_{\text{st},s,h1} = \eta^{\text{heat}}_{\text{st}} \times Q^{\text{heat}}_{\text{st},s,h24} + \eta^{\text{heat}}_{\text{st-in}} \times Q^{\text{heat}}_{\text{st-in},s,h24} - Q^{\text{heat}}_{\text{st-out},s,h24} / \eta^{\text{heat}}_{\text{st-out}} \quad \forall\, s \tag{8c}$$

$$0 \leqslant Q^{\text{heat}}_{\text{st-in},s,h} \leqslant \alpha^{\text{heat}}_{\text{chr},s,h} \times Q^{\text{limit}}_{\text{st-in}} \quad \forall\, s,h \tag{8d}$$

$$0 \leqslant Q^{\text{heat}}_{\text{st-out},s,h} \leqslant \alpha^{\text{heat}}_{dis,s,h} \times Q^{\text{limit}}_{\text{st-out}} \quad \forall\, s,h \tag{8e}$$

$$\alpha^{\text{heat}}_{\text{chr},s,h} + \alpha^{\text{heat}}_{dis,s,h} \leqslant 1 \quad \forall\, s,h \tag{8f}$$

where the stored heat as well as heat discharge and charge rates cannot exceed certain limits. Meanwhile, the stored heat in tank must return to the initial state at the end of each day; initial state is a degree of freedom, hence ensuring a cyclic steady state.

3.4.2. Battery

Battery is adopted, coupling with the solar PV panels, considering renewable energy intermittency. The electricity generated from PV panel can either be sent to fulfill demand or sent to store in the battery if needed [22]. Thus, the installed capacity of battery is set to be not less than that of PV. Meanwhile, surplus electricity generated by other devices can also be charged into the battery. Similar to thermal storage, the battery related formulas are displayed in Eq. (9), where three battery operation states, i.e., standby, charge, discharge, are constrained by Eqs. (9c)(9e) by another binary variable of α.

$$E^{\text{bat}}_{s,h} \leqslant CAP^{\text{limit}}_{\text{bat}} \quad \forall\, s,h \tag{9a}$$

$$E^{\text{bat}}_{s,h+1} = \eta^{\text{bat}}_{\text{st}} \times E^{\text{bat}}_{\text{st},s,h} + \eta^{\text{bat}}_{\text{st-in}} \times E^{\text{bat}}_{\text{st-in},s,h+1} - E^{\text{bat}}_{\text{st-out},s,h+1} / \eta^{\text{bat}}_{\text{st-out}} \quad \forall\, s,h \tag{9b}$$

$$0 \leqslant E^{\text{bat}}_{\text{st-in},s,h} \leqslant \alpha^{\text{bat}}_{\text{chr},s,h} \times E^{\text{limit}}_{\text{st-in}} \quad \forall\, s,h \tag{9c}$$

$$0 \leqslant E^{\text{bat}}_{\text{st-out},s,h} \leqslant \alpha^{\text{bat}}_{dis,s,h} \times E^{\text{limit}}_{\text{st-out}} \quad \forall\, s,h \tag{9d}$$

$$\alpha^{\text{bat}}_{\text{chr},s,h} + \alpha^{\text{bat}}_{dis,s,h} \leqslant 1 \quad \forall\, s,h \tag{9e}$$

3.5. Solar photovoltaic panel and thermal collector constraints

To improve the proposed systems' sustainability, installations of solar PV panel and vacuum tube thermal collector on the roof have been considered in this study. The solar PV power output is defined at Eq. (10) [22].

$$\eta_{\text{pv},s,h} = P_1 \times \left[\left(\frac{SRI_{s,h}}{SRI_0}\right)^{P_2} + P_3 \times \left(\frac{SRI_{s,h}}{SRI_0}\right) \right] \left[1 + P4 \times \left(\frac{T_{s,h}}{T_0}\right)^{P_2} + P_5 \times \frac{AM_{s,h}}{AM_0} \right] \quad \forall\, s,h \tag{10a}$$

$$E_{\text{pv},s,h} = A_{\text{pv}} \times \eta_{\text{pv},s,h} \times SRI_{s,h} \quad \forall\, s,h \tag{10b}$$

where the PV panel efficiency η_{pv} is related to solar radiation index (SRI) in the unit of (W/m^2), the ambient temperature (T), and the air mass (AM), $SRI_0 = 1000\ W/m^2$, $T_0 = 25\ ^\circ C$, $AM_0 = 1.5$, $P_1 = 0.2820$, $P_2 = 0.3967$, $P_3 = -0.4473$, $P_4 = -0.093$, $P_5 = 0.1601$.

The vacuum tube solar thermal collector model has been established by Eq. (11) [23].

$$\eta_{\text{tc}} = \eta_0 - a_1 \times \frac{(T'_{s,h} - T_0)}{SRI_{s,h}} - a_2 \times \frac{(T'_{s,h} - T_0)^2}{SRI_{s,h}} \quad \forall\, s,h \tag{11a}$$

$$Q_{tc,s,h} = A_{\text{tc}} \times \eta_{tc,s,h} \times SRI_{s,h} \quad \forall\, s,h \tag{11b}$$

where Q_{tc} is the heating supplied from thermal collector, η_{tc} is the solar thermal collector efficiency, $\eta_0 = 73\%$, $a_1 = 1.26$ and $a_2 = 0.004$ in unit of ($W/m^2\,K$), T' is the working fluid (water) temperature, A_{tc} is the solar thermal collector installed area.

Since the roof of each building has certain surface limit (assumed to be $500\ m^2$), the installation of thermal collector plus solar PV should within the limit.

$$Roof^{\text{limit}} \geqslant A_{\text{tc}} + A_{\text{pv}} \quad \forall\, s,h \tag{12}$$

3.6. Solid oxide fuel cell constraints

Solid Oxide Fuel Cell (SOFC) is the prime mover as well as the core of the CCHP system. To make the model closer to the real-world operation conditions, several unique constraints have been introduced as follows.

3.6.1. On/off constraint

The electrical output of SOFC is defined by the installed capacity (CAP_{fc}) multiplied by the part load ratio (PL_{fc}) at each time step and the fuel consumption ($Q^{\text{NG}}_{\text{fc}}$) can be calculated. The efficiency varies with the part-load ratio, which is empirical fitted as shown in Eq. (13) [24]. Furthermore, the on/off binary variable β is introduced, if the device is on ($\beta = 1$), the minimum output of this device should not lower than 30% of its installed capacity to avoid the device operating at very low load condition, and not higher than 100% of its installed capacity physically [25].

$$E_{\text{fc},s,h} = \beta_{\text{fc},s,h} \times CAP_{\text{fc}} \times PL_{\text{fc},s,h} \quad \forall\, s,h \tag{13a}$$

$$E_{fc,s,h} = \eta_{\text{fc},s,h} \times Q^{\text{NG}}_{\text{fc},s,h} \quad \forall\, s,h \tag{13b}$$

$$\eta_{\text{fc},s,h} = 0.494 \times (PL_{\text{fc},s,h})^3 - 1.196 \times (PL_{\text{fc},s,h})^2 + 0.945 \times PL_{\text{fc},s,h} + 0.236 \tag{13c}$$

$$PL_{\text{fc},s,h} \geqslant 30\% \times \beta_{\text{fc},s,h} \quad \forall\, s,h \tag{14a}$$

$$PL_{\text{fc},s,h} \leqslant 100\% \times \beta_{\text{fc},s,h} \quad \forall\, s,h \tag{14b}$$

3.6.2. Start limit constraint

In addition to the on/off constraint, a start limit constraint is also applied by introducing binary variable (φ) to avoid switching on and off the device frequently [26]. Thus, the constraint is particularly designed which only allows one time switching on and off the device each day. The constraint can be formulated as:

$$\sum_h \varphi_{\text{fc},s,h} \leqslant 1 \quad \forall\, h,s \tag{15a}$$

$$\varphi_{\text{fc},s,h+1} \geqslant \beta_{\text{fc},s,h+1} - \beta_{\text{fc},s,h} \quad \forall\, h,s \tag{15b}$$

$$\varphi_{\text{fc},s,h+1} \leqslant 1 - \beta_{\text{fc},s,h} \quad \forall\, h,s \tag{15c}$$

$$\varphi_{\text{fc},s,h+1} \leqslant \beta_{\text{fc},s,h+1} \quad \forall\, h,s \tag{15d}$$

3.6.3. Ramp up/down constraint

Another practical constraint of ramp up/down aims to limit the

power output variation between each time step so as to improve the lifetime of the device [27].

$$PL_{\mathrm{fc},s,h+1} - PL_{\mathrm{fc},s,h} \leqslant 50\% \quad \forall\, s,h \tag{16a}$$

$$PL_{\mathrm{fc},s,h1} - PL_{\mathrm{fc},s,h24} \leqslant 50\% \quad \forall\, s,h \tag{16b}$$

3.7. Objectives and evaluation criteria

In this study, two objectives of minimizing annual total cost (ATC) and annual carbon emissions (ACE) have been considered from economic and environmental perspectives. Meanwhile, the trade-off between them has been analyzed by bi-objective optimizations. Besides, the distributed energy system mismatch problem has also been quantified by introducing the criteria of on-site energy fraction (OEF) and on-site energy matching (OEM). The definitions of all objectives and criteria have been presented as follows.

3.7.1. Economic objective and criteria

The annual total cost (ATC) is defined as the economic objective, which consists of five parts: (1) the capital cost of each installed equipment, (2) the fuel cost from SOFC and boiler, (3) the maintenance cost of SOFC, battery, boiler, electrical chiller, absorption chiller, thermal storage, heat pump, solar PV and solar thermal collector, (4) the revenue of export electricity to grid, (5) the cost to purchase electricity from grid [28]. Thus, the *ATC* can be calculated as Eq. (17). Meanwhile, the sum of part (2) to (5) is defined as the operation cost (*OPEX*).

$$\begin{aligned} ATC = {} & CRF \times \sum_{t} CAP_t \times C^{\mathrm{CAP}} \quad \text{annualized capital cost} \\ & + \sum_{s,h} \left(\frac{E_{\mathrm{fc},s,h}}{\eta_{\mathrm{fc}}} + \frac{Q^{\mathrm{heat}}_{\mathrm{b},s,h}}{\eta_{\mathrm{b}}} \right) \times C_{NG} \quad \text{fuel cost} \\ & + \sum_{s,h} \left(E_{\mathrm{bat/pv/fc},s,h} + Q^{\mathrm{heat}}_{\mathrm{hp/tc/b/st},s,h} + Q^{\mathrm{cool}}_{\mathrm{ec/ac},s,h} \right) \times C^{\mathrm{maint}}_{t} \quad \text{maintenance cost} \\ & - C_{\mathrm{ex}} \times \sum_{s,h} E_{\mathrm{ex},s,h} \quad \text{export revenue} \\ & + C_{\mathrm{im}} \times \sum_{s,h} E_{im,s,h} \quad \text{grid electricity cost} \end{aligned} \tag{17}$$

$$CRF = \frac{r \times (1+r)^n}{(1+r)^n - 1} \tag{18}$$

where *CRF* is the capital recovery factor, *r* is the interest rate, *n* is the project life (years) [29].

Therefore, the economic criterion is defined as the OPEX saving (OPEXS) accordingly, as shown in Eq. (19).

$$OPEXS = \frac{OPEX_{\mathrm{base}} - OPEX_{\mathrm{CCHP}}}{OPEX_{\mathrm{base}}} \tag{19}$$

where the subscript of base and CCHP represent the baseline case and the proposed hybrid SOFC-CCHP system, respectively.

3.7.2. Environmental objective and criteria

The annual carbon emissions (ACE) is selected as the environmental objective which quantifies by the emissions from fuel consumed plus the electricity purchased from grid as defined in Eq. (20).

$$\begin{aligned} ACE = {} & \partial_{\mathrm{NG}} \times \sum_{s,h} \left(\frac{E_{\mathrm{fc},s,h}}{\eta_{\mathrm{fc}}} + \frac{Q^{\mathrm{heat}}_{\mathrm{b},s,h}}{\eta_{\mathrm{b}}} \right) \quad \text{natural gas emissions} \\ & + \partial_{\mathrm{grid}} \times \sum_{s,h} E_{im,s,h} \quad \text{purchased electricity emissions} \end{aligned} \tag{20}$$

where ∂_{NG} and ∂_{grid} are the emission factors of natural gas and grid, respectively.

Thus the environmental criteria of carbon emission saving (CES) can be defined as:

$$CES = \frac{ACE_{\mathrm{base}} - ACE_{\mathrm{CCHP}}}{ACE_{\mathrm{base}}} \tag{21}$$

3.7.3. Technical criteria

The technical criteria of on-site energy fraction (OEF) and on-site energy matching (OEM) have also been calculated [30,31]. The OEF is defined by the proportion of energy load fulfilled by the on-site generated energy to total demand, which indicates the independence of proposed system to the grid. The OEM is defined as the ratio of on-site generated energy that is used for load (rather than exported or dumped) to total on-site generated power, which represents the matchness between hybrid SOFC-CCHP system and the energy demand. In this case, these two ratios can be calculated by:

$$OEM = 50\% \times OEM_{\mathrm{ele}} + 50\% \times (OEM_{\mathrm{heat}} + OME_{\mathrm{cool}})/2 \tag{22a}$$

$$OEM_{\mathrm{ele}} = \frac{E_{\mathrm{pv}} + E_{\mathrm{fc}} - E_{\mathrm{ec}} - E_{\mathrm{ex}} - E_{\mathrm{hp}}}{E_{\mathrm{pv}} + E_{\mathrm{fc}}} \tag{22b}$$

$$OEM_{\mathrm{heat}} = \frac{Q^{\mathrm{heat}}_{\mathrm{demand}}}{Q^{\mathrm{heat}} + Q^{\mathrm{heat}}_{\mathrm{waste}}} \tag{22c}$$

$$OME_{\mathrm{cool}} = \frac{Q^{\mathrm{cool}}_{\mathrm{demand}}}{Q^{\mathrm{cool}} + Q^{\mathrm{cool}}_{\mathrm{waste}}} \tag{22d}$$

$$OEF = 50\% \times OEF_{\mathrm{ele}} + 50\% \times (OEF_{\mathrm{heat}} + OEF_{\mathrm{cool}})/2 \tag{23a}$$

$$OEF_{\mathrm{ele}} = \frac{E_{\mathrm{pv}} + E_{\mathrm{fc}} - E_{\mathrm{ec}} - E_{\mathrm{ex}} - E_{\mathrm{hp}}}{E_{\mathrm{demand}}} \tag{23b}$$

$$OEF_{\mathrm{heat}} = \frac{Q_{\mathrm{b}} + Q_{\mathrm{hp}} + Q_{\mathrm{tc}}}{Q^{\mathrm{heat}}_{\mathrm{demand}}} \tag{23c}$$

$$OMF_{\mathrm{cool}} = \frac{Q^{\mathrm{cool}}_{\mathrm{ec}} + Q^{\mathrm{cool}}_{\mathrm{ac}}}{Q^{\mathrm{cool}}_{\mathrm{demand}}} \tag{23d}$$

$$OEP = 50\% \times OEF + 50\% \times OEM \tag{24}$$

where the OEP (on-site energy performance) is defined by Eq. (24) as the technical criterion assessed in this study.

4. Multi-objective optimization and decision making

In this section, a multi-objective optimization method is introduced and three decision making approaches are described in detail accordingly.

4.1. Multi-objective optimization

Generally, a multi-objective model represents more than one objective. Since two objectives have been considered in this study, the problem can be named by multi-objective or bi-objective in this case. This study utilizes the $\mathcal{E}$-constraint approach to identify the non-dominated optimal solution set for multi-objective optimization [32]. For each objective, the most desired (Ideal) point and the least desired (Non-ideal) point can be determined through single objective optimizations, then one of the objectives can be discretized into several segments and converted to constraints [33]. Thus, another objective has to be optimized within the inequality constraints of the previous discretized objective. Previous studies have demonstrated that the optimal points identified are guaranteed global optimal points correspondingly [34]. In each case, the optimization results can be collected from the proposed model, then all feasible solutions would be displayed as a Pareto frontier as illustrated in Fig. 4. The next step is to identify the overall most desired solution by various decision making approaches.

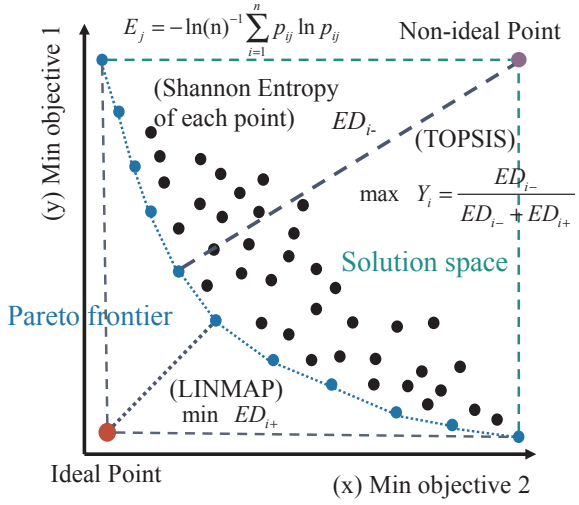

Fig. 4. Illustration of three decision making approaches.

4.2. Decision making

The optimal solution selection plays a vital role for multi-objective optimization. And the process is not that straightforward compared to single-objective optimization problems. Each Pareto-optimal solution represents a compromise considering different objectives, each component within the corresponding vector of objectives is non-dominated and cannot simultaneously be improved [35]. In this study, in order to verify and compare the effectiveness of different decision making approaches, three well-known approaches of LINMAP (Linear Programming Technique for Multidimensional Analysis of Preference) [36], TOPSIS (Technique for Order of Preference by Similarity to Ideal Solution) [37] and Shannon Entropy [38] have been applied, which are based on two types of mechanisms. A brief illustration is presented in Fig. 4.

4.2.1. Linear Programming Technique for Multidimensional Analysis of Preference

Taking a two-objective minimization problem for example, all feasible solutions are distributed in the solution space, including the Pareto optimal solutions (in blue) and non-Pareto solutions (in black), as shown in Fig. 4. The blue points form the Pareto frontier, and each of them is non-dominated but dominates other points who are not Pareto optimal solutions (in black). During the Linear Programming Technique for Multidimensional Analysis of Preference (LINMAP) decision process, the "Ideal" point is introduced and located at the best place of the search space. Since the optimal value of single-objective optimizations is impossible to achieve through multi-objective optimization, the ideal point is not on the Pareto frontier. By LINMAP approach, the Euclidian distance (ED_{i+}) between each point on Pareto frontier and ideal point is defined in Eq. (25), thus the point on Pareto frontier with the shortest distance is considered as the prior optimal point. More details about LINMAP approach is provided in Refs. [35–37].

$$ED_{i+} = \sqrt{\sum_{j=1}^{n} (f_{ij}^{\text{norm}} - f_j^{\text{ideal}})^2} \tag{25}$$

where i denotes the index of each solution on the Pareto frontier, and j is the index of the objective considered.

4.2.2. Technique for Order Preference by Similarity to an Ideal Solution

By Technique for Order Preference by Similarity to an Ideal Solution (TOPSIS) approach, the "Non-ideal" point is also introduced, which the latitude and longitude is determined by two blue endpoints on the Pareto frontier as presented in Fig. 4. Compared to the Ideal point, the Non-ideal point is on the opposite side of the Pareto frontier. Thus, the Euclidian distance (ED_{i-}) between each point on Pareto frontier and the Non-ideal point can be calculated as shown in Eq. (26). Then, a new assessment (Y_i) is introduced as Eq. (27), and the solution with maximum Y_i is considered as the most desired solution [35].

$$ED_{i-} = \sqrt{\sum_{j=1}^{n} (f_{ij}^{\text{norm}} - f_j^{\text{nadir}})^2} \tag{26}$$

$$Y_i = \frac{ED_{i-}}{ED_{i-} + ED_{i+}} \tag{27}$$

4.2.3. Shannon entropy

Shannon entropy is proposed by Shannon to quantify the uncertainty of the source of information [2,14]. A larger value of Shannon entropy for certain information represents larger uncertainty, which further means the weight of this information should be lower. In this case, the objectives are the information, thus the problem is to assign normalized weights to each objective. Based on the Shannon entropy theory, the entropy value of j objective can be calculated by Eqs. (28) and (29), where i represents each solution. Then the weight of each objective (θ_j) is obtained by Eq. (30). Furthermore, a comprehensive decision making index of S_i is expressed in Eq. (31). Since the less of ATC and ACE, the better, which means the solution with minimum S_i value is considered as the final desired solution.

$$H_j = -c\sum_{i=1}^{m} h_{ij}\ln h_{ij}; \quad (1 \leqslant j \leqslant n) \tag{28}$$

$$c = \frac{1}{\ln m}; \quad h_{ij} = \frac{f_{ij}}{\sum_{i=1}^{m} f_{ij}} \tag{29}$$

$$\theta_j = \frac{1-H_j}{n-\sum_{j=1}^{n} H_j}; \quad (j = 1,2,\ldots,n); \quad \sum_{j=1}^{n} \theta_j = 1 \tag{30}$$

$$S_i = f_{ij} \times \theta_j; \quad i_{final} = i \in \min(S_i) \tag{31}$$

Note that for all three decision making approaches, the solutions on the Pareto frontier should be normalized by Eqs. (32) or (33) [39].

$$f_{ij}^{\text{norm}} = \frac{f_{ij} - \min(f_{ij})}{\max(f_{ij}) - \min(f_{ij})} \tag{32}$$

$$f_{ij}^{\text{norm}} = \frac{\max(f_{ij}) - f_{ij}}{\max(f_{ij}) - \min(f_{ij})} \tag{33}$$

In order to give an insight into various solutions, as well as compare the most desired solution identified by different decision making approaches, a deviation index (d) is also introduced in Eq. (34) [35,37,39].

$$d = \frac{\sqrt{\sum_{j=1}^{n} (f_j - f_j^{\text{ideal}})^2}}{\sqrt{\sum_{j=1}^{n} (f_j - f_j^{\text{ideal}})^2} + \sqrt{\sum_{j=1}^{n} (f_j - f_j^{\text{nadir}})^2}} \tag{34}$$

5. Evaluation approach description

In this study, the proposed hybrid SOFC-CCHP systems have been applied to both hospital and hotel in three different locations, which can be defined as six cases. Among each case, three scenarios are considered including two single-objective optimal solutions and one bi-objective optimal solution with minimum deviation index. Meanwhile several dimensionless criteria from economic, environmental and technical perspectives have been proposed for comparison purposes. In order to identify which location and building type is the best site for demonstration of such a system, the problem can be induced as a comprehensive evaluation issue. Previous research has demonstrated that the multi-criteria fuzzy evaluation approaches are effective to solve

this type of problem [2,16,17]. Therefore, an integrated assessment model has been built by combination of the Analytic Hierarchy Process approach (AHP) and the Gray Relation Analysis (GRA) approaches in this study. By the proposed assessment model, the system performance is evaluated considering the criteria from different perspectives with various scales simultaneously. Meanwhile, the AHP approach assigns weights of each criterion in a subjective manner indicating the decision-makers or experts' judgement [17], and the weights are further revised by the GRA approach to make to selection more objective [16]. The process of integrated evaluation is described as follows.

Step 1: Establish a pair-wise comparison matrix.

To determine the relative importance of each criterion, the first step is to construct the hierarchical structure of the problem and further establish the pair-wise comparison matrix based on the experts' scoring of each criterion. The scoring is within the range of 1 to 9, where score of 1 represents two criteria with equal importance, whereas score of 9 indicates one criterion is much more important than the other one [40]. After scoring by experts, an original comparison matrix can be written as:

$$B = \begin{vmatrix} b_{11} & b_{12} & \cdots & b_{1n} \\ b_{21} & b_{22} & \cdots & b_{2n} \\ \vdots & \vdots & \vdots & \vdots \\ b_{n1} & b_{n2} & \cdots & b_{nn} \end{vmatrix}; \quad 0 \leqslant b_{ij} \leqslant 9; \quad b_{ji} = \frac{1}{b_{ij}}; \quad b_{ii} = 1 \tag{35}$$

where n is the number of criteria.

Step 2: Test the consistency.

Due to the subjectivity of the experts' scoring, the pair-wise comparison matrix's consistency needs to be tested by the index of consistency ratio (CR), where a CR value less of 0.1 is considered acceptable, whereas a new pair-wise comparison matrix is required by rescoring the weight of each criteria. The equation to calculate the CR value is shown in Eq. (36), where consistency index (CI) value can be calculated by Eq. (37) and a random consistency index (RI) value has been pre-determined based on the order of the matrix (equal to 0.58 in this work) [40].

$$CI = \frac{\lambda_{\max} - n}{n-1} \tag{36}$$

$$CR = \frac{CI}{RI} \tag{37}$$

where $\lambda_{\max}$ is the maximum eigenvalue of the matrix,

Step 3: Calculate the weight of each criterion by using AHP approach.

Once the original matrix passes the test of consistency, it can be normalized as shown in Eq. (38), then the weight vector can be obtained by Eq. (39).

$$W = \begin{vmatrix} w_{11} & w_{12} & \cdots & w_{1n} \\ w_{21} & w_{22} & \cdots & w_{2n} \\ \vdots & \vdots & \vdots & \vdots \\ w_{n1} & w_{n2} & \cdots & w_{nn} \end{vmatrix}; \quad w_{ji} = \frac{a_{ij}}{\sum_{i=1}^{n} a_{ij}} \tag{38}$$

$$q_j = \frac{\sum_{j=1}^{n} w_{ij}}{n}; \quad Q = [q_1 \;\; q_2 \;\; \cdots \;\; q_n]^T \tag{39}$$

Step 4: Standardize initial matrix and determine the reference sequence.

Assuming the problem involves m cases and n criteria, the initial matrix can be written as Eq. (40).

$$X = \begin{bmatrix} x_{11} & x_{12} & \cdots & x_{1n} \\ x_{21} & x_{22} & \cdots & x_{2n} \\ \vdots & \vdots & \vdots & \vdots \\ x_{m1} & x_{m2} & \cdots & x_{mn} \end{bmatrix}, \quad (1 \leqslant i \leqslant m, 1 \leqslant j \leqslant n) \tag{40}$$

In order to eliminate the adverse effect of different ranges and units of each criterion, the initial matrix needs to be standardized. Usually, the criteria can be grouped into two types: "the higher, the better" such as efficiency and "the lower, the better" such as simple payback period. By linear transformation of Eqs. (41) and (42), the initial matrix can be standardized while not changing the proportional relationship of the original data as illustrated in Eq. (43).

$$\text{For the higher, the better: } r_{ij} = \frac{x_{ij} - \min\limits_{1 \leqslant j \leqslant n} x_{ij}}{\max\limits_{1 \leqslant j \leqslant n} x_{ij} - \min\limits_{1 \leqslant j \leqslant n} x_{ij}}, \quad (1 \leqslant i \leqslant m, 1 \leqslant j \leqslant n) \tag{41}$$

$$\text{For the lower, the better: } r_{ij} = \frac{\max\limits_{1 \leqslant j \leqslant n} x_{ij} - x_{ij}}{\max\limits_{1 \leqslant j \leqslant n} x_{ij} - \min\limits_{1 \leqslant j \leqslant n} x_{ij}}, \quad (1 \leqslant i \leqslant m, 1 \leqslant j \leqslant n) \tag{42}$$

where r_{ij} is the element of the standardized matrix.

As shown in Eqs. (43) and (44), the matrix R is the standardized matrix, and $R^{\max}$ represents the reference sequence, each element $r_{0j}^{\max}$ is the maximum value of j column elements.

$$R = \begin{bmatrix} r_{11} & r_{12} & \cdots & r_{1n} \\ r_{21} & r_{22} & \cdots & r_{2n} \\ \vdots & \vdots & \vdots & \vdots \\ r_{m1} & r_{m2} & \cdots & r_{mn} \end{bmatrix}, \quad (1 \leqslant i \leqslant m, 1 \leqslant j \leqslant n) \tag{43}$$

$$\begin{aligned} R^{\max} &= [r_{01}^{\max} \;\; r_{02}^{\max} \;\; \cdots \;\; r_{0n}^{\max}] \\ r_{0j}^{\max} &= \max(r_{1j}, r_{2j}, \cdots, r_{ij}, \cdots, r_{mj}) \end{aligned} \tag{44}$$

Step 5: Calculate gray incidence coefficient.

The Gray Incidence Coefficient is defined as the proximal degree of the standardized matrix to the reference sequence which can be calculated by Eq. (45):

$$\lambda_{ij} = \frac{\min\limits_{i=1}^{m}\left[\min\limits_{j=1}^{n}(r_{ij} - r_{0j}^{\max})\right] + \theta \cdot \max\limits_{i=1}^{m}\left[\max\limits_{j=1}^{n}(r_{ij} - r_{0j}^{\max})\right]}{(r_{ij} - r_{0j}^{\max}) + \theta \cdot \max\limits_{i=1}^{m}\left[\max\limits_{j=1}^{n}(r_{ij} - r_{0j}^{\max})\right]}, \quad (1 \leqslant i \leqslant m, 1 \leqslant j \leqslant n) \tag{45}$$

where λ_{ij} refers to the gray incidence coefficient value and θ is the distinguishing coefficient, which is always assumed to be 0.5 [40].

Step 6: Determine integrated gray incidence degree and overall priority.

The integrated gray incidence degree of each case (p_{0i}) can be calculated by multiplying the weight degree of each criterion (q_j) obtained from Step 3 with the gray incidence coefficient value λ_{ij} from Step 5, as illustrated in Eq. (46), Each p_{0i} is a value within 0–1. Finally, the integrated gray incidence degree of each case can be expressed as a single column matrix of P. By descending the order of integrated gray incidence degree for each case, the overall priority of all cases can be determined based on the ranking order.

$$p_{0i} = \sum_{j=1}^{n} \omega_j \cdot \lambda_{ij}(j), \quad (1 \leqslant i \leqslant m, \; 1 \leqslant j \leqslant n) \tag{46}$$

$$P = (p_{01}, p_{02}, \cdots, p_{0i}, \cdots, p_{0m})^T, \quad (1 \leqslant i \leqslant m) \tag{47}$$

6. Case study

In this section, the proposed model and evaluation approaches are applied to a series of case studies. Two types of building, hospital and hotel, are applied in the case studies, considering their relatively stable daily energy demand as well as their own representative demand characteristics. Meanwhile, three locations, i.e., Beijing, Shanghai and Xiamen of China, are selected to represent three different climate zones, i.e., 'Cold', 'Hot summer, cold winter' and 'Hot summer, warm winter', respectively. Each climate has strong impact on the heating and cooling demands of buildings. Therefore, overall six case studies are conducted with significant differences in climate conditions, energy demand profiles, energy prices and carbon emissions. Fig. 5(a–c) shows the typical electrical, heating and cooling demand of a year for a hospital in Shanghai as a representative, in which spring and fall are considered as the transition seasons, thus a year can be divided to three periods: summer, winter and transition season. Meanwhile, Fig. 5(d–f) illustrates the typical energy demand for a hotel in Shanghai. A significant difference can be seen from the two buildings' energy profiles (1) the peak load period of the hospital and the hotel is different, (2) The hotel has a relatively steady load compared to the hospital. Although the prediction of the demand profile is a challenging problem, in this work the focus is the optimization model and evaluation approach, thus the hourly energy demand profiles of a typical day during three periods are considered as the representative energy demand over corresponding period. Meanwhile, the energy prices as well as the electrical feed-in prices of each selected city have been presented in Fig. 5(g–i).

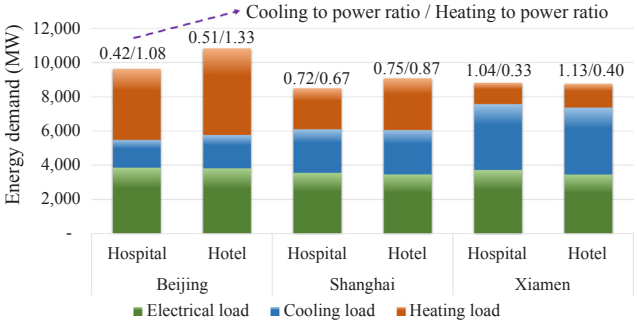

Fig. 6. Energy demand characteristics of hospital and hotel in different cities.

In order not to lose the generality, the hospitals and hotels with comparable scale and similar electrical demand in each location have been considered. The annual energy demand breakdown as well as the heating/cooling to power ratio is illustrated in Fig. 6. It can be seen that the buildings in Beijing have a larger heating demand and less cooling demand. On the contrary, the heating demand is small and the cooling demand is high for the buildings in Xiamen. Besides, heating and cooling demand are both moderate in Shanghai compared to the other two locations.

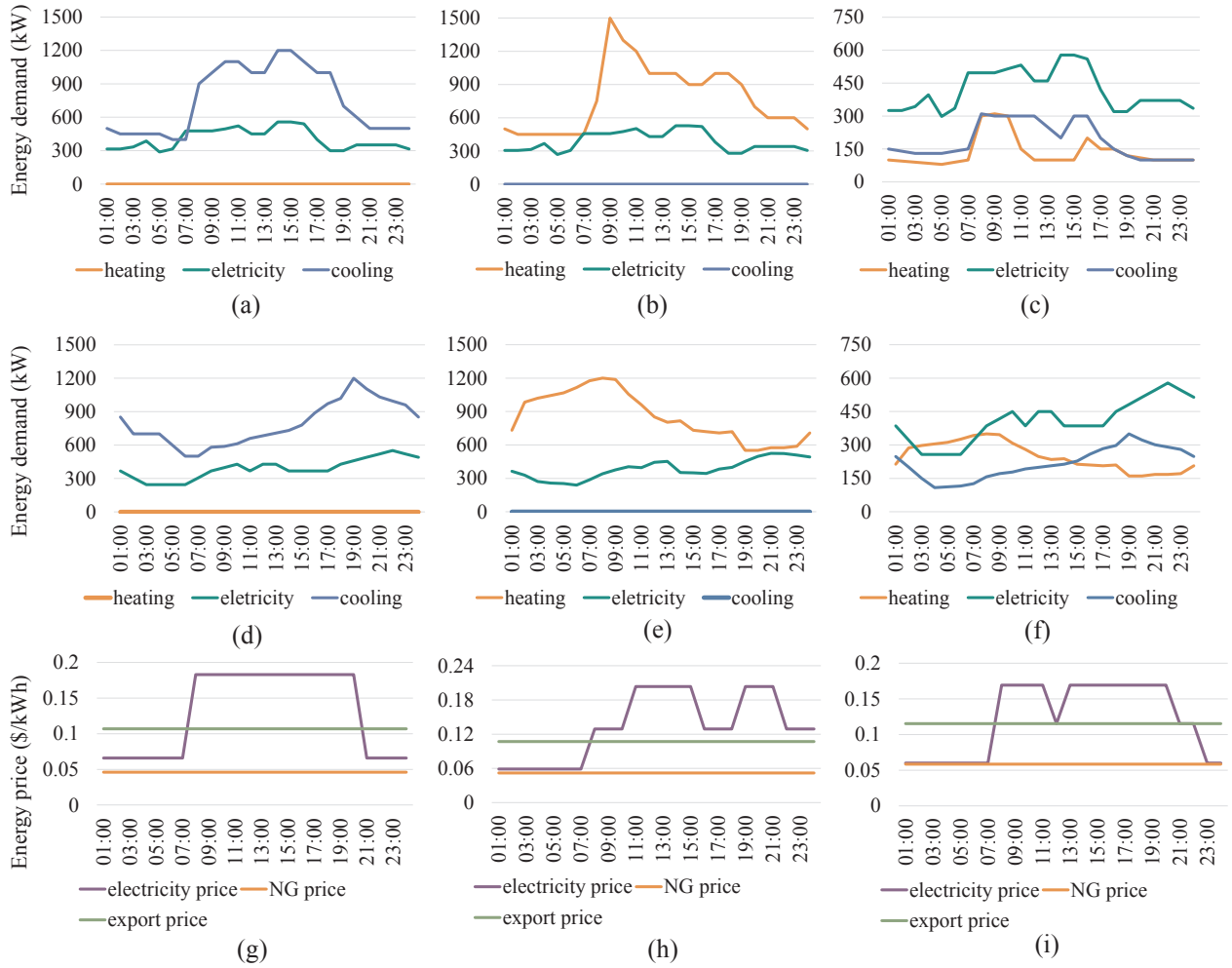

Fig. 5. Summer (a, d) winter (b, e) transition (c, f) energy demand of hospital (a–c) and hotel (d–f) in Shanghai and the energy prices of Shanghai (g) Beijing (h) and Xiamen (i).

6.1. Input parameters

Based on our model, the state-of-the-art technical, economic and environmental input parameters have been given in this section. Table 1 lists the general project assumptions as well as the carbon emission factors, where the selected cities are assumed with same natural gas emission factor and different grid emission factors.

The technical input parameters of SOFC, boiler, absorption chiller, electrical chiller, heat pump, heat exchanger and heat storage with assumptions have been presented in Table 2. It is assumed that the SOFC stack substitution happens per 5 years, and the stack replacement cost of 1200 $/kW has been added up to the capital cost [41]. Meanwhile, the upper bounds of installed capacity for each device are listed in Table 2 as well, and the value for solar PV panel and thermal collector are limited by the installation space as described in Eq. (12).

Climate data have significant impact on the performance of the solar PV and the thermal collector. In this study, the solar radiation indexes and the outdoor air temperatures of selected cities are presented in Fig. 7.

In addition, the capital cost and maintenance cost of major devices are listed in Table 3, where capital cost is proportional to the installed capacity, and maintenance cost is related to the energy produced.

7. Results and discussion

In this study, the proposed MINLP model is developed in GAMS 24.0 [46] on a PC with an Intel (R) Core (TM) i5-4590 CPU, 3.30 GHz CUP and 8.0 GB of RAM, and the results are solved by the LINDO solver [47].

7.1. Pareto frontiers

The Pareto optimal frontiers of each case are displayed in Fig. 8. For each Pareto frontier, the single-objective optimal points, and the bi-objective optimal points have been particularly marked with letters,

- Letters A, B, C, D, E, F represent the case of Shanghai-hospital (a), Shanghai-hotel (b), Beijing-hospital (c), Beijing-hotel (d), Xiamen-hospital (e), Xiamen-hotel (f) respectively.
- Number 1, 2, 3, 4, 5 indicate the scenario to achieve the least ATC objective, the least ACE objective, and the bi-objective optimization solutions identified by LINMAP, TOPSIS, and Shannon Entropy, respectively.

There is a clear trade-off between two objectives for all cases. In order to achieve a lower ATC, the ACE will increase slowly at first and then rise up significantly. Different cases show similar trade-off tendency, though the varying degrees are different. To better understand the relation between ATC and ACE, cubic curves with high R^2 (Coefficient of correlation) values are fitted based on the optimized points located on corresponding Pareto frontiers, hence the fitting formulations are displayed in Table 4.

7.2. Decision making

Fig. 8 also illustrates the bi-objective optimal solutions identified by different decision making approaches for all cases. It can be observed that the bi-objective optimal solutions identified by the LINMAP and TOPSIS decision making approaches are always consistent and located on the intermediate section of the Pareto frontiers as marked in points by number 3 and 4 in (a) to (f). This phenomenon can be explained by the convex type of Pareto frontiers obtained in this study. Meanwhile, both two decision making approaches are calculated based on the Eulerian distance, thus the middle section of points tend to be closer to the "ideal" point, which make them the most desired solution and both LINMAP and TOPSIS approaches make no significant difference.

However, it can be also observed that the optimal solutions (number 5) identified by the Shannon Entropy approach are different from LINMAP/TOPSIS approaches in most of the cases except for case B. Meanwhile, the gaps between Shannon Entropy and the LINMAP/TOPSIS also vary case by case. As the Shannon Entropy approach is based on the uncertainty of information, it can be reflected in terms of curvature of the obtained Pareto frontiers in this study. By plotting six cases' Pareto frontiers together as shown in Fig. 9, it is seen that if the curvature is relatively constant during the entire Pareto frontier, then both two objectives are assigned with similar weights, which further lead to the identified bi-objective optimal point falling to the intermediate section of the Pareto frontier. This situation occurred in Figs. 8(b) and 9 both marked in orange, in which the optimal point identified is consistent for all three decision making approaches. While in other cases, the weights of two objectives are somehow different, thus the optimal points identified will be partial to a certain side as expected for Shannon Entropy method.

In order to make further comparison of three decision making approaches, the details of three decision making approaches as well as the deviation index (d) have been presented in Fig. 10. The optimal solutions identified for each case have been particularly marked for LINMAP and TOPSIS (in red), and Shannon Entropy (in black) approaches.

It is observed from Fig. 10 that the LINMAP and TOPSIS approaches tend to have a smaller value of deviation index (d) than the Shannon Entropy approach, which may indicate that the decision making approach based on the Eulerian distance is more suitable in present study. Therefore, in the rest of this paper, the solution selected by LINMAP/TOPSIS is considered as the representative of the final desired solution for bi-objective optimal design and dispatch of the hybrid SOFC-CCHP system.

7.3. Technical performance

Table 5 lists the design installed capacities of all devices for representative cases. For each case, five scenarios have been considered, which presents two single objective optimal solutions and three bi-objective optimal solutions identified by different decision making approaches. Significant differences can be observed when different objectives are considered in each case, and several patterns have been observed as follows,

In general, to achieve the minimum annual total cost (ATC), the installed capacities of SOFC tend to be slightly less than other scenario due to the high capital cost of SOFC for all cases. Meanwhile, the installed capacities of absorption chiller are less than other scenario as well due to the relatively low energy efficiency. By contrast, larger capacities of electrical chiller have been installed as the COP of electrical chiller is significantly higher. In order to achieve the minimum annual carbon emission (ACE), SOFC installed capacities tend to be larger due to its lower emission features compared to the grid. Meanwhile, larger capacities of absorption chiller would be applied for

Table 1
Project general information and emission factors [3,16].

Parameters		Value	Unit
Project lifetime		10	years
Interest rate		6	%
Natural gas emission factor (∂_{NG})	Beijing	0.18	kg/kWh (LHV)
	Shanghai	0.18	kg/kWh (LHV)
	Xiamen	0.18	kg/kWh (LHV)
Grid electricity emission factor (∂_{grid})	Beijing	1.01	kg/kWh
	Shanghai	0.95	kg/kWh
	Xiamen	1.00	kg/kWh

Table 2
Technical input parameters of major component [5,42,43].

System	Parameters	Value	Unit
SOFC	System rated efficiency (η_{fc})	48%	
	Daily start limit (φ)	1	
	Maximum capacity (CAP_{fc}^{limit})	580	kW
	Stack lifetime	5	years
Boiler	Efficiency (η_{b})	85%	
	Maximum capacity (CAP_{b}^{limit})	1500	kW
Absorption chiller	Efficiency (η_{ac})	100%	
	Maximum capacity (CAP_{ac}^{limit})	1200	kW
Electrical chiller	Coefficient of performance (η_{ec})	400%	
	Maximum capacity (CAP_{ec}^{limit})	1200	kW
Heat pump	Coefficient of performance (η_{hp})	350%	
	Maximum capacity (CAP_{hp}^{limit})	1200	kW
Heat exchanger	Efficiency (η_{hex})	90%	
Solar PV	Efficiency (η_{pv})	Eqs. (10a) and (10b)	
Thermal collector	Efficiency (η_{tc})	Eqs. (11a) and (11b)	
Battery	In-storage efficiency (η_{st}^{bat})	97%	
	Battery charge efficiency (η_{st-in}^{bat})	95%	
	Battery discharge efficiency (η_{st-out}^{bat})	95%	
	Maximum capacity (CAP_{bat}^{limit})	150	kW
Heat storage	In-storage efficiency (η_{st}^{heat})	95%	
	Heat charge efficiency (η_{st-in}^{heat})	95%	
	Heat discharge efficiency (η_{st-out}^{heat})	95%	
	Maximum capacity (CAP_{st}^{limit})	1000	kW

the ability to recover the heat waste heat. Boiler and electrical chiller installed capacities are not only effected by the optimization objectives but also highly dependent on the climate zones (i.e., heating and cooling demand differences). Overall, in the solutions of bi-objective optimization, the installed capacities of most of the devices are somewhere between two single objective optimizations An interesting finding is that solar PV + battery system are preferred than solar thermal collectors (STC) in terms of solar energy utilization in most of the cases, except for the cases in Xiamen, where both solar availability and heating demand are relatively lower. This is the outcome of multiple factors such as cost, energy efficiencies, preferred objectives, as well as demand and climate conditions. Cost might be the major contributor, which is also consistent with the rapid development momentum of solar PV industry currently as the capital cost of such renewable technology has been falling, although, further in-depth study is required. Meanwhile, coupled with the PV panel, battery is adopted in each cases. The electricity price difference between off-peak purchasing and peak feed-in cannot make enough profit to offset the capital cost of battery based on the tariff assumptions in present study. Thus, the battery maintains its “buffer” effect for the system, while not turning into a profitable means.

Another significant finding is that hotel hardly needs thermal storage compared to the hospital, except for the case of Beijing with minimal cost objective. This phenomenon may be explained by two reasons, (1) the energy demand of the hotel is more stable than that of the hospital over 24 h in general, which makes the energy storage not necessary; (2) each type of energy demand is supplied by more than one technology, thus certain combinations of different supply devices are enough to handle the variation demand without thermal storage.

7.4. Economic performance

In this section, the economic performance assessment is presented, and the bi-objective optimal solution with the lowest deviation index (d) has been selected as the representative of the corresponding desired solution for each case as mentioned. Firstly, the energy performance baseline of each case is presented in Table 6, where the electrical, cooling and heating demand of each building is fulfilled by the grid, electrical chiller, and natural gas boiler respectively.

Fig. 11 demonstrates the 10-year project life cost breakdown comparison of each case and scenario as well as the levelized cost of energy (LCOE). In general, SOFC fuel cost and capital cost are the two biggest contributors due to the high capital cost of SOFC as well as its merit energy conversion efficiency. Meanwhile, bought electricity accounts for a significant amount in ‘Min ATC’ scenarios when significant amounts of electricity would be imported during the off-peak low price period so as to fulfill the demand with the least cost. In addition, the scenarios aiming to achieve the lowest annual total cost (ATC) have the lowest LCOE among three different scenarios as expected with a small

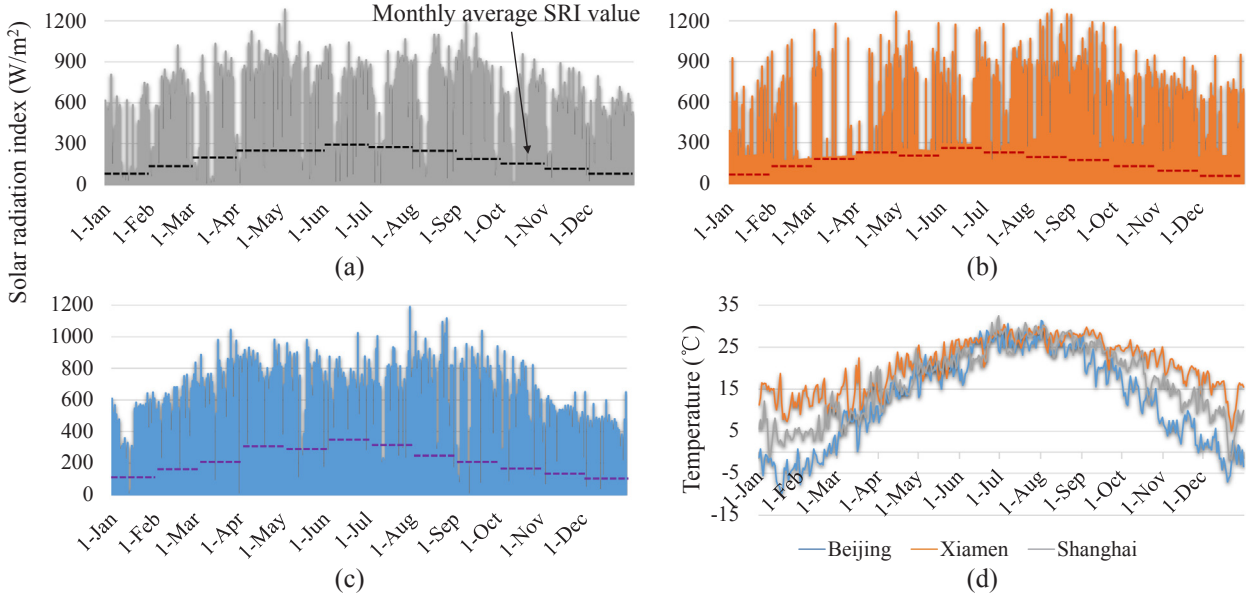

Fig. 7. Climate data inputs of solar radiation indexes of Beijing (a) Xiamen (b) Shanghai (c) and the outdoor air temperatures (d).

Table 3
Economic input parameters of major components.

Device	Capital cost (C^{cap}) $/kW	Maintenance cost (C^{maint}) $/kWh
SOFC [11,41]	3900	0.005
Boiler [22,7]	50	0.0003
Absorption chiller [22,7]	230	0.002
Electrical chiller [7,22]	150	0.002
Heat storage [7,22]	25	0.0003
Heat pump [11]	200	0.002
Solar PV [7,44]	750	0.002
Solar thermal collector [22,23]	200	0.001
Battery [7,45]	1075	0.003

portion of feed-in revenue. It is also seen from the climate zone perspective that the implementation of proposed hybrid SOFC-CCHP systems in Beijing and Shanghai can achieve a competitive LCOE compared to the baseline system which may make such cutting-edge technology possible to penetrate the market in the near future. However, Xiamen is not a desirable location for demonstration of such system and the main reason is the large cooling load and small heating load of its climate condition. Since the existing cooling supply by electrical chiller already has a good coefficient of performance (COP), even though the proposed system recovered and cascade utilized the heat along with power generation, the operation cost saving is not enough to offset the high capital cost of new technologies. Therefore, the location with large amount of heating demand and medium amount of cooling demand is recommended for demonstrate such system.

7.5. Environmental performance

The annual carbon emissions (ACE) of all cases and scenarios as well as the baseline condition are illustrated in Fig. 12. In general, a significant amount of carbon emissions can be saved by implementing the proposed hybrid SOFC-CCHP system. Considering different objectives, the aims of 'Min ACE' achieve the highest carbon emission savings as expected with larger capacities of sustainable energy devices. By contrast, in order to reduce annual total cost (ATC), significant amounts of electricity have to be purchased from the grid during the low price period which have a negative impact on the carbon emission reduction significantly. Besides, the emissions for bi-objective scenarios lie between two single objective optimizations. From the climate zone perspective, the average carbon emissions saving calculated from two buildings and three scenarios are 54%, 56% and 60% for Shanghai, Beijing and Xiamen respectively, which may be explained by the lower dependence on boilers while maximizing the reliance on SOFC power supply. As for the building categories, two types of building in Beijing have similar carbon emission reductions (56%) considering the average saving rate of three scenarios. It is also seen that the hotel achieves a larger carbon reduction rate than the hospital does both in Shanghai and Xiamen. Note that above observations are based on the assumption that the electricity coming from grid is with a relatively high emission factor considering the coal-fired power still accounts for a portion of electricity mix in China. The results may vary when the assumption changes.

7.6. Multi-criteria evaluation

Based on the technical, economic and environmental assessment results, a multi-criteria assessment model has been built to identify the overall optimal location and building type as well as the most desired scenario simultaneously. Ten experts have been invited to evaluate the relative importance among these three criteria, then the weights of three criteria have been calculated using the Analytic Hierarchy Process (AHP) method as described in Section 5. Note that the weights from the AHP method may be different depending on the motivation of the experts or decision-makers [18]. Furthermore, the Grey Relation Analysis (GRA) approach is applied to modify the weights and calculate the integrated gray incidence degree of all cases and scenarios, thus the final synthetic score and ranking can be determined.

Table 7 provides the original input data to the multi-criteria assessment model. For the operation cost saving (OPEXS), Beijing achieves slightly better savings than Shanghai and significantly better than Xiamen. The main reason is the larger heating demand in the northern climate zone, the proposed system can significantly improve the heating supply efficiency which leads to the operation cost

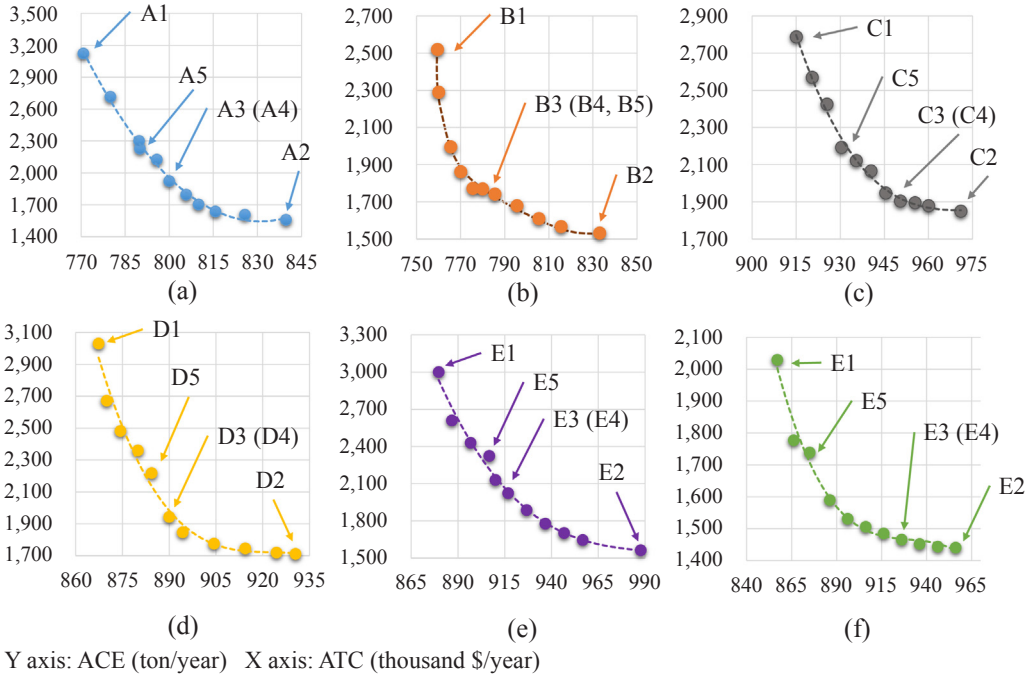

Fig. 8. Pareto frontiers with marked optimal solutions - case Shanghai hospital (a), Shanghai hotel (b), Beijing hospital (c), Beijing hotel (d), Xiamen hospital (e), Xiamen hotel (f).

Table 4
Fitted formulas between the ACE and ATC for each case.

Case	Fitted curve formulation	R^2 value	ATC range (in 10^3 $)
Shanghai – hospital	$ACE = -8 \times 10^{-12} \times ATC^3 + 2 \times 10^{-5} \times ATC^2 - 15.78 \times ATC + 4 \times 10^6$	0.989	775–836
Shanghai – hotel	$ACE = -1 \times 10^{-11} \times ATC^3 + 2 \times 10^{-5} \times ATC^2 - 19.46 \times ATC + 5 \times 10^6$	0.981	755–823
Beijing – hospital	$ACE = -3 \times 10^{-12} \times ATC^3 - 9 \times 10^{-6} \times ATC^2 + 8.59 \times ATC - 3 \times 10^6$	0.984	910–969
Beijing – hotel	$ACE = -4 \times 10^{-12} \times ATC^3 - 1 \times 10^{-5} \times ATC^2 - 9.61 \times ATC + 3 \times 10^6$	0.989	864–928
Xiamen – hotel	$ACE = -5 \times 10^{-13} \times ATC^3 - 1 \times 10^{-6} \times ATC^2 - 1.50 \times ATC + 5.16 \times 10^5$	0.991	877–987
Xiamen – hotel	$ACE = -1 \times 10^{-12} \times ATC^3 - 4 \times 10^{-6} \times ATC^2 - 3.29 \times ATC + 1 \times 10^6$	0.986	857–956

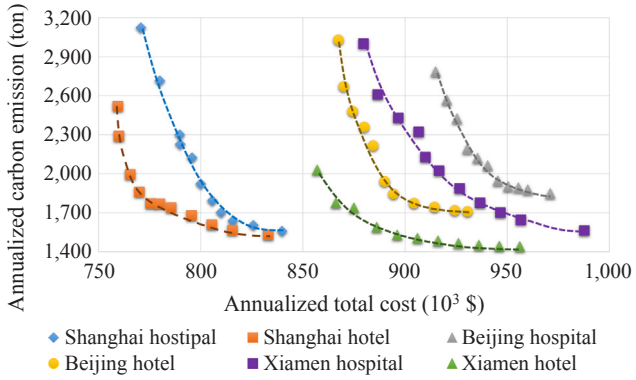

Fig. 9. Summary of Pareto frontiers for six cases.

reductions compared to the baseline system. Meanwhile, the objective of minimizing annual carbon emission (ACE) achieves the highest carbon emission saving (CES) in all cases as expected. In addition, it is also observed that the system achieves best (OEP) with the objective to minimize ACE.

The final scores and rankings of all cases and scenarios are summarized in Fig. 13. It can be seen that the proposed hybrid SOFC-CCHP system implemented in Beijing achieves the overall best performance in general, slightly higher than Shanghai and significantly better than Xiamen due to the efficient heating supply and corresponding operation cost saving. Meanwhile, the hotel seems to be more suitable for demonstrating the proposed system than the hospital for all three locations which may be explained by more steady energy demand, less low-load situation and higher efficiency of onsite power generation accordingly. In each case, the scenarios with the objective to achieve minimum annual carbon emission (ACE) turn out to be the better choice than other scenarios, since the emission saving is significant and the energy is more independent to the grid with slightly sacrifice on the cost compared to the else two scenarios. In addition, the top three scenarios have been identified to provide guidance to investors and decision makers, and such observation is the result of synthesized factors including climate conditions, energy prices, and demand characters, etc.

8. Conclusion

This study proposes a combined multi-objective optimization and multi-criteria evaluation framework for optimal planning of distributed energy system. The system multi-objective optimal design and dispatch is from the technical perspective, while the multi-criteria evaluation is more from the marketing perspective. Such combination can provide a comprehensive evaluation framework, which is particularly useful for evaluating a new technology or system. To validate the effectiveness of

Case	Shanghai hostipal					Shanghai hotel					Beijing hostipal				
			Shannon Entropy					Shannon Entropy					Shannon Entropy		
Solution number	LINMAP (ED_{i+})	TOPSIS (Y_i)	Final value	weights of ATC/ACE	deviation index (d)	LINMAP (ED_{i+})	TOPSIS (Y_i)	Final value	weights of ATC/ACE	deviation index (d)	LINMAP (ED_{i+})	TOPSIS (Y_i)	Final value	weights of ATC/ACE	deviation index (d)
1	1.000	0.500	0.082	0.393/0.607	0.976	1.000	0.500	0.087	0.411/0.589	0.986	1.000	0.500	0.050	0.283/0.717	0.984
2	0.835	0.537	0.076		0.832	0.888	0.530	0.078		0.887	0.848	0.536	0.049		0.847
3	0.669	0.600	0.064		0.666	0.744	0.563	0.077		0.740	0.771	0.559	0.049		0.769
4	0.579	0.633	0.063		0.570	0.613	0.604	0.078		0.592	0.687	0.591	0.046		0.685
5	0.525	0.650	0.067		0.500	0.491	0.663	0.074		0.444	0.609	0.617	0.052		0.600
6	0.475	0.669	0.074		0.404	0.434	0.696	0.072		0.362	0.565	0.617	0.073		0.516
7	0.510	0.640	0.090		0.333	0.382	0.730	0.066		0.296	0.520	0.636	0.081		0.431
8	0.515	0.645	0.094		0.238	0.396	0.723	0.075		0.215	0.504	0.644	0.092		0.346
9	0.533	0.645	0.096		0.167	0.490	0.672	0.091		0.148	0.667	0.555	0.138		0.262
10	0.793	0.546	0.134		0.073	0.766	0.557	0.134		0.067	0.785	0.525	0.165		0.166
11	1.000	0.500	0.162		0.024	1.000	0.500	0.168		0.014	1.000	0.500	0.204		0.016

Case	Beijing hotel					Xiamen hostipal					Xiamen hotel				
			Shannon Entropy					Shannon Entropy					Shannon Entropy		
Solution number	LINMAP (ED_{i+})	TOPSIS (Y_i)	Final value	weights of ATC/ACE	deviation index (d)	LINMAP (ED_{i+})	TOPSIS (Y_i)	Final value	weights of ATC/ACE	deviation index (d)	LINMAP (ED_{i+})	TOPSIS (Y_i)	Final value	weights of ATC/ACE	deviation index (d)
1	1.000	0.500	0.069	0.344/0.656	0.980	1.000	0.500	0.093	0.427/0.573	0.987	1.000	0.500	0.049	0.269/0.731	0.994
2	0.935	0.516	0.065		0.932	0.730	0.574	0.076		0.727	0.899	0.527	0.046		0.899
3	0.780	0.562	0.058		0.778	0.644	0.602	0.073		0.636	0.798	0.556	0.044		0.798
4	0.625	0.621	0.052		0.623	0.565	0.631	0.072		0.545	0.699	0.590	0.046		0.697
5	0.479	0.686	0.051		0.467	0.507	0.651	0.074		0.455	0.601	0.627	0.049		0.596
6	0.436	0.700	0.060		0.399	0.485	0.657	0.079		0.364	0.508	0.668	0.054		0.496
7	0.495	0.651	0.092		0.312	0.497	0.650	0.083		0.303	0.423	0.711	0.060		0.395
8	0.549	0.624	0.108		0.244	0.594	0.593	0.099		0.273	0.388	0.726	0.082		0.294
9	0.605	0.609	0.119		0.156	0.629	0.591	0.101		0.182	0.538	0.640	0.144		0.182
10	0.734	0.565	0.141		0.088	0.734	0.564	0.110		0.091	0.578	0.635	0.157		0.092
11	1.000	0.500	0.185		0.020	1.000	0.500	0.140		0.013	1.000	0.500	0.267		0.006

Fig. 10. Details and deviation index of different decision making processes.

Table 5
Comparison of system design between different cases using three decision makings and single objective optimizations.

Case	Objective	Decision making	Optimal value		Design installed capacity							
			ATC (10^3 $)	ACE (ton)	SOFC (kW_e)	Boiler (kW_h)	EC (kW_e)	AC (kW_c)	HP (kW_e)	PV + Battery (kW_e)	STC (m^{2-})	Tank (kW_h)
Shanghai-Hospital	Min ATC	–	770	3124	471	810	300	0	215	75	0	0
	Min ACE	–	839	1559	574	710	170	560	295	75	0	457
	Bi-objective	LINMAP	805	1924	501	784	229	286	223	75	0	0
		TOPSIS										
		Shannon Entropy	813	1704	505	790	200	350	240	75	0	0
Shanghai-Hotel	Min ATC	–	759	2520	452	747	300	0	222	75	0	0
	Min ACE	–	833	1532	574	354	172	520	240	75	0	0
	Bi-objective	LINMAP	779	1775	475	735	137	253	230	70	45	0
		TOPSIS										
		Shannon Entropy										
Beijing-Hospital	Min ATC	–	915	2767	545	201	167	184	334	80	0	120
	Min ACE	–	971	1941	570	629	58	706	204	80	0	520
	Bi-objective	LINMAP	930	2193	558	1040	169	175	221	80	0	290
		TOPSIS										
		Shannon Entropy	950	1904	563	810	101	602	210	80	0	430
Beijing-Hotel	Min ATC	–	867	3030	465	37	224	0	376	80	0	178
	Min ACE	–	930	1714	572	575	400	538	285	45	157	0
	Bi-objective	LINMAP	890	1943	548	282	168	225	283	50	78	0
		TOPSIS										
		Shannon Entropy	894	1846	553	310	201	300	284	53	85	0
Xiamen-Hospital	Min ATC	–	879	3001	432	0	339	201	129	25	238	0
	Min ACE	–	988	1564	585	0	218	650	40	65	0	0
	Bi-objective	LINMAP	917	2025	480	0	263	348	94	34	207	0
		TOPSIS										
		Shannon Entropy	937	1778	500	0	240	450	86	42	152	0
Xiamen-Hotel	Min ATC	–	858	2041	471	0	218	307	93	26	264	0
	Min ACE	–	956	1441	600	0	165	767	24	65	0	0
	Bi-objective	LINMAP	886	1590	463	0	201	375	82	28	254	0
		TOPSIS										
		Shannon Entropy	936	1452	590	0	172	705	31	33	207	0

Table 6
Baseline energy performance of each case.

Case	Installed capacity (kW)		Cost breakdown ($/year)					OPEX (10^3 $/year)	LCOE ($/kWh)	Carbon emission (ton/year)
	Boiler	Electrical chiller	Heating	Electricity	Cooling	Maintenance	Annualized capital			
Shanghai-Hospital	2000	1500	129,771	486,980	94,790	5931	44,168	717,473	0.142	4490
Shanghai-Hotel	1500	1500	163,915	457,840	88,173	6249	40,770	716,176	0.139	4550
Beijing-Hospital	2500	900	253,914	549,811	58,469	4718	35,334	866,913	0.146	5185
Beijing-Hotel	1800	950	288,835	514,939	67,966	5410	31,597	877,150	0.154	5008
Xiamen-Hospital	900	1800	85,029	480,497	131,008	8165	42,809	704,699	0.141	4882
Xiamen-Hotel	900	1800	95,077	432,441	124,437	8320	42,809	660,275	0.138	4729

the proposed framework, an optimal planning case study of a solar assisted solid oxide fuel cell based CCHP system in different buildings located at different climate zones is conducted. Several conclusions can be drawn as follows,

- From the case study, the relation between cost and emission objectives can be well fitted to cubic curves with high R^2 value (i.e., over 0.98) for the ease of engineers and decision makers to evaluate the trade-off between optimal cost and optimal emissions. More importantly, the best demonstration site and building type are also identified by subjective and objective combined evaluation method. All these results can provide quantitative guidance for the

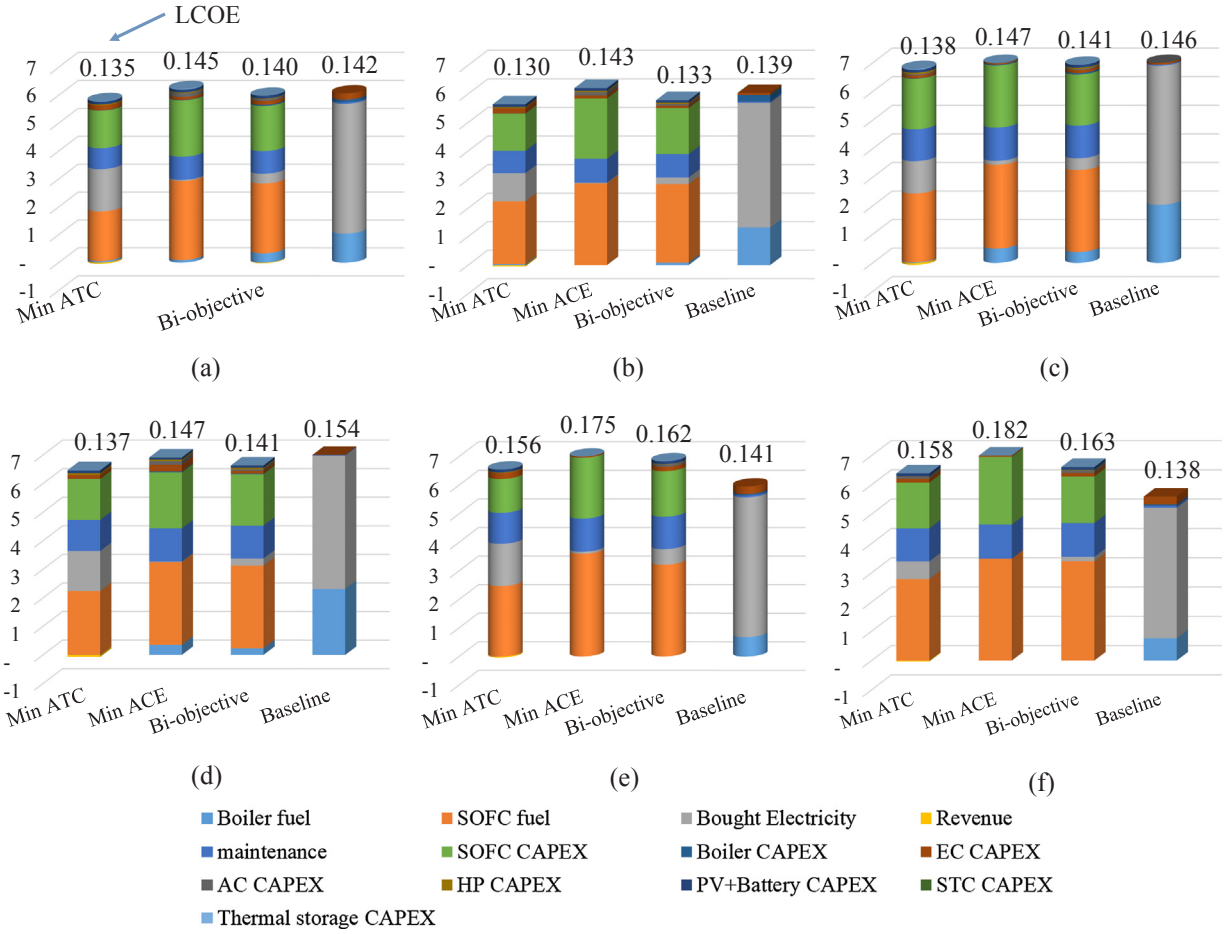

Fig. 11. Project total cost breakdown and LCOE comparison - case of Shanghai hospital (a), Shanghai hotel (b), Beijing hospital (c), Beijing hotel (d), Xiamen hospital (e), Xiamen hotel (f).

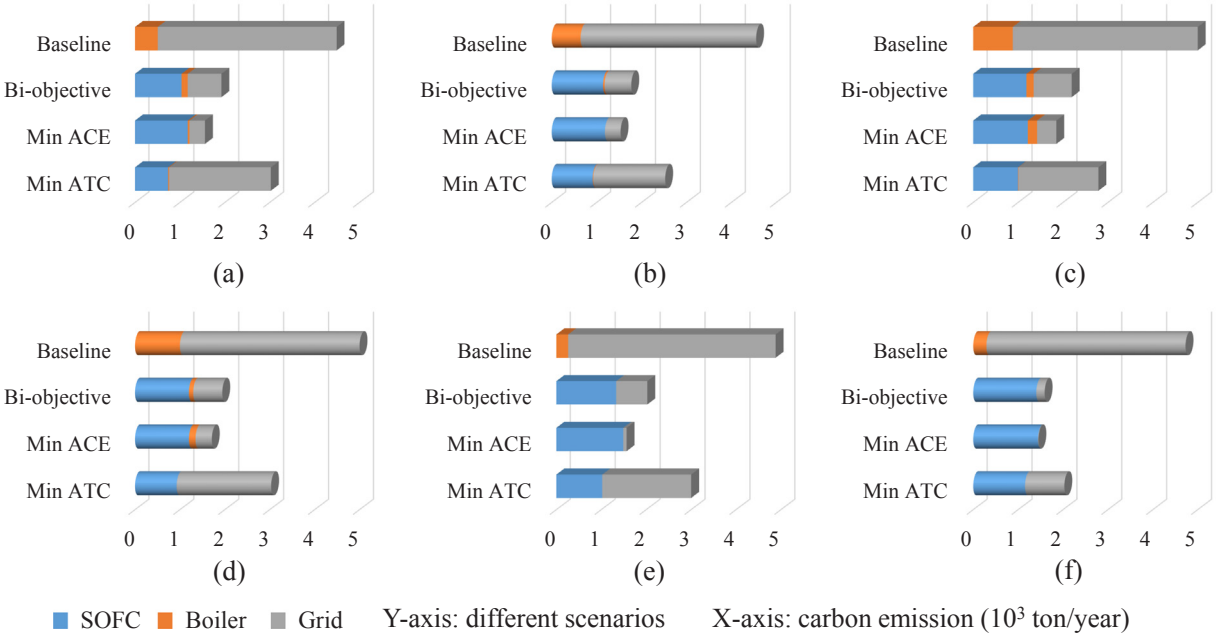

Fig. 12. Carbon emission comparison with the baselines - case of Shanghai hospital (a), Shanghai hotel (b), Beijing hospital (c), Beijing hotel (d), Xiamen hospital (e), Xiamen hotel (f).

Table 7
Original data for multi-criteria assessment.

Criteria	Shanghai-Hospital			Shanghai-Hotel			Beijing-Hospital		
	Min ATC	Min ACE	Bi-objective	Min ATC	Min ACE	Bi-objective	Min ATC	Min ACE	Bi-objective
OPEXS*	24%	29%	25%	26%	31%	28%	28%	27%	26%
CES*	33%	65%	57%	45%	66%	61%	46%	64%	58%
OEP*	68%	92%	89%	76%	93%	89%	77%	92%	87%
Criteria	Beijing-Hotel			Xiamen-Hospital			Xiamen-Hotel		
	Min ATC	Min ACE	Bi-objective	Min ATC	Min ACE	Bi-objective	Min ATC	Min ACE	Bi-objective
OPEXS	28%	33%	31%	5%	9%	7%	9%	6%	5%
CES	39%	66%	61%	39%	68%	59%	57%	69%	66%
OEP	67%	91%	87%	77%	94%	87%	86%	95%	92%

* OPEXS – operation cost saving, CES – carbon emission saving, OEP – on-site energy performance.

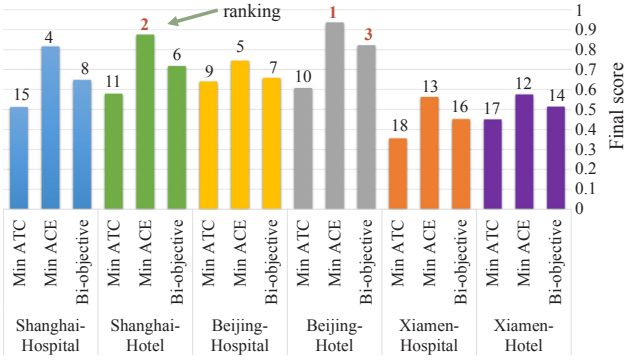

Fig. 13. Final score and overall ranking of all cases and scenarios.

demonstration of stationary Solid Oxide Fuel Cell technology in China.

- Three decision making approaches in multi-objective optimization have been compared. LINMAP and TOPSIS approaches tend to be more suitable for this research with a smaller value of deviation index (d) compared to Shannon Entropy approach. This observation is based on two objective-optimization, and the Pareto curves are convex and smooth. When the curvature remain relatively constant on the whole Pareto frontiers, the final desired solution obtained by each approach would be identical.
- It is also observed that solar PV + battery is preferred instead of solar thermal collectors in most cases and scenarios as solar energy utilization alternatives, which is the results from various factors (e.g., cost, efficiency, demand, and climate). This observation is also consistent with the rapid development of PV and battery industry currently as well as the significant drop on PV and battery capital cost. On the other hand, the overall system performance has been evaluated comprehensively by the proposed framework. The ranking of climate zones is Beijing > Shanghai > Xiamen, and the ranking of building types is hotel > hospital, while the ranking of objectives is Min ACE > Bi-objective > Min ATC. The top three scenarios for demonstrating the SOFC technology are also identified, which are as follows: hotel in Beijing with Min ACE objective, hotel in Shanghai with Min ACE, and hotel in Beijing with bi-objective optimization.
- It is noteworthy that the optimal and evaluation results are case specific based on the inputs and assumptions of the present study, but the modelling and evaluation approaches are applicable to other distributed energy systems applied in various conditions. Future research may involve more evaluation indexes (e.g., system reliability) in the framework.

Acknowledgement

The work was supported by National Natural Science Foundation of China under grant No. 51206137.

References

[1] Leobner I, Smolek P, Heinzl B, Raich P, Schirrer A, Kozek M, et al. Simulation-based strategies for smart demand response. J Sustain Dev Energy Water Environ Syst 2017;6:33–46.
[2] Li M, Mu H, Li N, Ma B. Optimal design and operation strategy for integrated evaluation of CCHP (combined cooling heating and power) system. Energy 2016;99:202–20.
[3] Huda ASN, Zivanovic R. Large-scale integration of distributed generation into distribution networks: Study objectives, review of models and computational tools. Renew Sustain Energy Rev 2017;76:974–88. http://dx.doi.org/10.1016/j.rser.2017.03.069.
[4] Ramadhani F, Hussain MA, Mokhils H, Hajimolana S. Optimization strategies for solid oxide fuel cell (SOFC) application: a literature survey. Renew Sustain Energy Rev 2017;76:460–84.
[5] Chen H, Yang C, Deng K, Zhou N, Wu H. Multi-objective optimization of the hybrid wind/solar/fuel cell distributed generation system using Hammersley Sequence Sampling. Int J Hydrogen Energy 2017;42:7836–46.
[6] Nojavan S, Majidi M, Zare K. Optimal scheduling of heating and power hubs under economic and environment issues in the presence of peak load management. Energy Convers Manage 2018;156:34–44.
[7] Luo Z, Wu Z, Li Z, Cai H, Li B, Gu W. A two-stage optimization and control for CCHP microgrid energy management. Appl Therm Eng 2017;125:513–22.
[8] Jin M, Feng W, Liu P, Marnay C, Spanos C. MOD-DR: microgrid optimal dispatch with demand response. Appl Energy 2017;187:758–76.
[9] Ma T, Wu J, Hao L. Energy flow modeling and optimal operation analysis of the micro energy grid based on energy hub. Energy Convers Manage 2017;133:292–306.
[10] Kang L, Yang J, An Q, Deng S, Zhao J, Wang H, et al. Effects of load following operational strategy on CCHP system with an auxiliary ground source heat pump considering carbon tax and electricity feed in tariff. Appl Energy 2017;194:454–66.
[11] Facci AL, Cigolotti V, Jannelli E, Ubertini S. Technical and economic assessment of a SOFC-based energy system for combined cooling, heating and power. Appl Energy 2017;192:563–74.
[12] Soheyli S, Shafiei Mayam MH, Mehrjoo M. Modeling a novel CCHP system including solar and wind renewable energy resources and sizing by a CC-MOPSO algorithm. Appl Energy 2016;184:375–95.
[13] Zhang D, Evangelisti S, Lettieri P, Papageorgiou LG. Economic and environmental scheduling of smart homes with microgrid: DER operation and electrical tasks. Energy Convers Manage 2016;110:113–24.
[14] Ju L, Tan Z, Li H, Tan Q, Yu X, Song X. Multi-objective operation optimization and evaluation model for CCHP and renewable energy based hybrid energy system driven by distributed energy resources in China. Energy 2016;111:322–40.
[15] Wei D, Chen A, Sun B, Zhang C. Multi-objective optimal operation and energy coupling analysis of combined cooling and heating system. Energy 2016;98:296–307.
[16] Wu Q, Ren H, Gao W, Ren J. Multi-criteria assessment of building combined heat and power systems located in different climate zones: Japan-China comparison. Energy 2016;103:502–12.
[17] Wang J-J, Jing Y-Y, Zhang C-F, Zhang X-T, Shi G-H. Integrated evaluation of distributed triple-generation systems using improved grey incidence approach. Energy 2008;33:1427–37.
[18] China meteorological data sharing service system. < http://data.cma.cn > [access: 2017/07/01].
[19] Zhang S, Liu H, Liu M, Sakaue E, Li N, Zhao Y. An efficient integration strategy for a SOFC-GT-SORC combined system with performance simulation and parametric

optimization. Appl Therm Eng 2017;121:314–24.
[20] Mehr AS, Mahmoudi SMS, Yari M, Chitsaz A. Thermodynamic and exergoeconomic analysis of biogas fed solid oxide fuel cell power plants emphasizing on anode and cathode recycling: a comparative study. Energy Convers Manage 2015;105:596–606.
[21] Moradi M, Mehrpooya M. Optimal design and economic analysis of a hybrid solid oxide fuel cell and parabolic solar dish collector, combined cooling, heating and power (CCHP) system used for a large commercial tower. Energy 2017;130:530–43.
[22] Wang J, Lu Y, Yang Y, Mao T. Thermodynamic performance analysis and optimization of a solar-assisted combined cooling, heating and power system. Energy 2016;115:49–59.
[23] Delgado-Torres AM, García-Rodríguez L. Analysis and optimization of the low-temperature solar organic Rankine cycle (ORC). Energy Convers Manage 2010;51:2846–56.
[24] US DOE hydrogen and fuel cells program: DOE fuel cell power analysis. FC power model solid oxide fuel cell, version 2.0. 2017. < https://www.gams.com/latest/docs/userguides/index.html > [access: 2017/07/01].
[25] Dodds PE, Staffell I, Hawkes AD, Li F, Grünewald P, McDowall W, et al. Hydrogen and fuel cell technologies for heating: a review. Int J Hydrogen Energy 2015;40:2065–83.
[26] Sorace M, Gandiglio M, Santarelli M. Modeling and techno-economic analysis of the integration of a FC-based micro-CHP system for residential application with a heat pump. Energy 2017;120:262–75.
[27] Napoli R, Gandiglio M, Lanzini A, Santarelli M. Techno-economic analysis of PEMFC and SOFC micro-CHP fuel cell systems for the residential sector. Energy Build 2015;103:131–46.
[28] Eriksson ELV, Gray EM. Optimization and integration of hybrid renewable energy hydrogen fuel cell energy systems – a critical review. Appl Energy 2017;202:348–64.
[29] Bracco S, Dentici G, Siri S. Economic and environmental optimization model for the design and the operation of a combined heat and power distributed generation system in an urban area. Energy 2013;55:1014–24.
[30] Zheng CY, Wu JY, Zhai XQ, Wang RZ. Impacts of feed-in tariff policies on design and performance of CCHP system in different climate zones. Appl Energy 2016;175:168–79.
[31] Cao S, Hasan A, Sirén K. On-site energy matching indices for buildings with energy conversion, storage and hybrid grid connections. Energy Build 2013;64:423–38.
[32] De-León Almaraz S, Azzaro-Pantel C, Montastruc L, Boix M. Deployment of a hydrogen supply chain by multi-objective/multi-period optimisation at regional and national scales. Chem Eng Res Des 2015;104:11–31.
[33] Fazlollahi S, Becker G, Ashouri A, Maréchal F. Multi-objective, multi-period optimization of district energy systems: IV – a case study. Energy 2015;84:365–81.
[34] Cui Y, Geng Z, Zhu Q, Han Y. Review: Multi-objective optimization methods and application in energy saving. Energy 2017;125:681–704.
[35] Li Y, Liao S, Liu G. Thermo-economic multi-objective optimization for a solar-dish Brayton system using NSGA-II and decision making. Int J Electr Power Energy Syst 2015;64:167–75.
[36] Ahmadi MH, Sayyaadi H, Dehghani S, Hosseinzade H. Designing a solar powered Stirling heat engine based on multiple criteria: maximized thermal efficiency and power. Energy Convers Manage 2013;75:282–91.
[37] Feng Y, Hung T, Zhang Y, Li B, Yang J, Shi Y. Performance comparison of low-grade ORCs (organic Rankine cycles) using R245fa, pentane and their mixtures based on the thermoeconomic multi-objective optimization and decision makings. Energy 2015;93:2018–29.
[38] Ahmadi MH, Ahmadi MA, Bayat R, Ashouri M, Feidt M. Thermo-economic optimization of Stirling heat pump by using non-dominated sorting genetic algorithm. Energy Convers Manage 2015;91:315–22.
[39] Feng Y, Zhang Y, Li B, Yang J, Shi Y. Comparison between regenerative organic Rankine cycle (RORC) and basic organic Rankine cycle (BORC) based on thermo-economic multi-objective optimization considering exergy efficiency and levelized energy cost (LEC). Energy Convers Manage 2015;96:58–71.
[40] Tang Y, Sun H, Yao Q, Wang Y. The selection of key technologies by the silicon photovoltaic industry based on the Delphi method and AHP (analytic hierarchy process): case study of China. Energy 2014;75:474–82.
[41] McLarty D, Brouwer J, Ainscough C. Economic analysis of fuel cell installations at commercial buildings including regional pricing and complementary technologies. Energy Build 2016;113:112–22.
[42] Zeng R, Li H, Jiang R, Liu L, Zhang G. A novel multi-objective optimization method for CCHP–GSHP coupling systems. Energy Build 2016;112:149–58.
[43] Wei M, Smith SJ, Sohn MD. Experience curve development and cost reduction disaggregation for fuel cell markets in Japan and the US. Appl Energy 2017;191:346–57.
[44] He YX, Pang YX, Li XM, Zhang MH. Dynamic subsidy model of photovoltaic distributed generation in China. Renew Energy 2018;118:555–64.
[45] Abdin GC, Noussan M. Electricity storage compared to net metering in residential PV applications. J Cleaner Prod 2018;176:175–86.
[46] GAMS Development Corporation. GAMS - a user's guide; 2017. < https://www.gams.com/latest/docs/userguides/index.html > [access: 2017/07/01].
[47] LINDO Systems Inc. LINDO API – user manual; 2017. < http://www.lindo.com/index.php/help/user-manuals > [access: 2017/07/01].